

LipoTag: A minimal motif for live and functional imaging of plant cell membranes.

Supplementary information

Table of contents

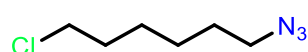
Synthetic procedures LipoTag precursors, fluorophore precursors and LipoTag modified fluorophores	2-8
Figure S1, staining of Arabidopsis with commonly used mammalian membrane probes and LipoTag dye precursors	9
Figure S2, concentration range FM4-64 in different Arabidopsis root zones	10
Figure S3, penetration depth of FM4-64 in different tissues over time	11
Figure S4, effect of staining concentration of non-functional LipoTag probes on tissue penetration after 30 minutes	12
Figure S5, staining kinetics of LipoTag-Green in the root tip and elongation zone	13
Figure S6, staining kinetics of LipoTag-Orange in the root tip and elongation zone	14
Figure S7, staining kinetics of LipoTag-Red in the root tip and elongation zone	15
Figure S8, chemical structures of non-functional LipoTag probes	16
Figure S9, plasmolysis of LipoTag stained Arabidopsis roots	17
Figure S10, staining of Arabidopsis roots with LipoTag-Cy5 and LipoTag-Oxa.	18
Figure S11, staining of <i>F. serratus</i> with LipoTag probes	19
Figure S12, staining of <i>Ectocarpus</i> with LipoTag probes	20
Figure S13, staining of <i>S. rigidula</i> with LipoTag probes	21
Figure S14, staining of <i>S. latissima</i> with LipoTag probes	22
Figure S15, staining of Murine macrophage cells with LipoTag dyes	23
Figure S16, staining of plasmodesmata in <i>Marchantia gemmae</i>	24
Figure S17, calibration of LipoTag-BDP	25
Figure S18, staining of Arabidopsis root with NR12S	26
Figure S19, mock hemin treatment with LipoTag-Ox	27
Figure S20, chemical structures of functional LipoTag probes	28
Figure S21, normalized fluorescence spectra of all LipoTag probes	29
Table S1, number of samples	30-31
Figure S22-45, NMR-spectra	32-55

LipoTag fluorophore conjugation, LipoTag and LipoTag precursors synthesis

LipoTag fluorophore general conjugation protocol.

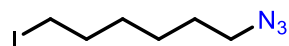
10 mg of alkyne modified fluorophore was dissolved in 4.5 ml DMF. CuSO_4 and THPTA were added from a 10mM and 5 mM stock solution in water so their final concentration is 200 and 500 μM respectively. 2 equivalents of LipoTag were added (compared to fluorophore) from a 100 mM stock solution in water. The resulting solution was stirred and bubbled with N_2 before the addition of sodium ascorbate from a 10 mM stock solution in water so its final concentration is 400 μM . The resulting mixture is left stirring overnight before being concentrated under air flow. The resulting product was run over a basic alumina plug, first washing with 10:90 MeOH/DCM followed by elution with 100% MeOH.

1-azido-6-chlorohexane (1)



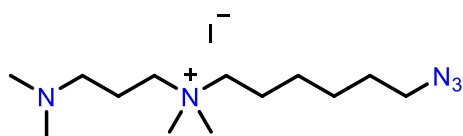
1-bromo-6-chlorohexane (6.9 ml, 46.2 mmol) was dissolved in 50 ml DMF. NaN_3 (3g, 46.2 mmol) was added and the mixture left to stir overnight at room temperature. The mixture was diluted with 60 ml of H_2O and the product extracted with 3x 75 Et_2O . The combined organic layers were washed with 3x100 ml H_2O . The organic layer was dried with MgSO_4 and concentrated under reduced pressure, yielding 6.99 g of **1** as an oil. Yield: 94%. **$^1\text{H NMR}$** (400 MHz, CDCl_3) δ 3.53 (t, J = 6.6 Hz, 2H), 3.27 (t, J = 6.9 Hz, 2H), 1.83 – 1.73 (m, 2H), 1.65 – 1.56 (m, 2H), 1.51 – 1.35 (m, 4H). **$^{13}\text{C NMR}$** (101 MHz, CDCl_3) δ 51.33, 44.90, 32.41, 28.73, 26.43, 26.04.

1-azido-6-iodohexane (2)



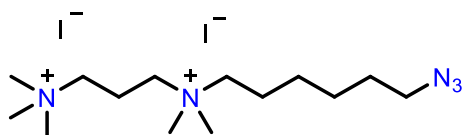
1 (6.9 g, 42.7 mmol) and NaI (12.77 g, 85.2 mmol) were added to 200 ml acetone. The mixture was bubbled with N_2 for 10 minutes and then left stirring for 24h under reflux. After cooling the mixture was diluted with 100 ml H_2O and extracted with 3x 100 ml EtOAc . The combined organic layers were dried with MgSO_4 and concentrated under vacuum, yielding 5.88g of **2**. Yield: 54%. **$^1\text{H NMR}$** (400 MHz, CDCl_3) δ 3.26 (t, J = 6.9 Hz, 2H), 3.18 (t, J = 6.9 Hz, 2H), 1.88 – 1.72 (m, 2H), 1.66 – 1.53 (m, 2H), 1.51 – 1.32 (m, 4H). **$^{13}\text{C NMR}$** (101 MHz, CDCl_3) δ 51.31, 33.24, 30.00, 28.67, 25.67, 6.77.

6-azido-N-(3-(dimethylamino)propyl)-N,N-dimethylhexan-1-aminium (3)



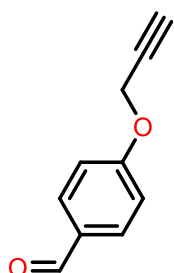
2 (800 mg, 3.2 mmol) and N,N,N',N'-tetramethyl-1,3-propanediamine (15 ml, 90 mmol) were dissolved in 40 ml of dry THF and left stirring overnight at room temperature. The mixture was concentrated under vacuum at 50 °C and washed three times with Et₂O and dried under vacuum yielding 1.12 g of **4**. Yield: 91%. ¹H NMR (400 MHz, MeOD) δ 3.43 – 3.32 (m, 6H), 3.11 (s, 6H), 2.41 (t, J = 7.1 Hz, 2H), 2.28 (s, 6H), 1.99 – 1.88 (m, 2H), 1.85 – 1.74 (m, 2H), 1.69 – 1.58 (m, 2H), 1.57 – 1.38 (m, 4H). ¹³C NMR (101 MHz, D₂O) δ 64.70, 64.14, 62.09, 54.76, 50.99, 50.81, 43.72, 27.74, 27.70, 25.50, 25.45, 25.03, 21.91, 21.80, 19.77.

LipoTag (4)



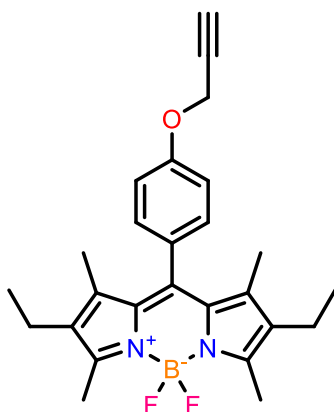
3 (400 mg, 1.04 mmol) was added to 5 ml of DMF followed by 2 ml of MeI (31 mmol). The mixture was left stirring overnight at room temperature and then concentrated under vacuum at 50 °C and washed with Et₂O yielding 508 mg of **4** as a viscous, brown oil. Yield: 93%. ¹H NMR (400 MHz, D₂O) δ 3.52 – 3.34 (m, 9H), 3.24 (s, 9H), 3.18 (s, 6H), 2.37 (s, 2H), 1.84 (s, 2H), 1.66 (s, 2H), 1.47 (s, 4H). ¹³C NMR (101 MHz, D₂O) δ 64.89, 62.48, 60.06, 53.36, 51.00, 34.57, 27.74, 25.49, 25.02, 21.90, 17.19.

4-(prop-2-yn-1-yloxy)benzaldehyde (**5**)



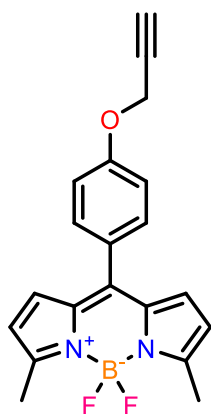
4-hydroxy-benzaldehyde (**3g**, 24.6 mmol) was dissolved in 250 ml of acetone. K_2CO_3 (13.58g, 98.3 mmol) and propargyl bromide (10.5 ml from a 80% solution with toluene, 98.3 mmol) were added and the mixture was bubbled with N_2 for 5 minutes. The mixture was heated to reflux for 4 hours, cooled to room temperature and diluted with 250 ml H_2O (all residual K_2SO_3 needs to be dissolved). The aqueous solution was extracted with 3x 200 ml DCM, the combined organic layers were dried with $MgSO_4$ and concentrated under vacuum, yielding 3.6g of **5** as a brown solid. Yield: 91%. 1H NMR (400 MHz, $CDCl_3$) δ 9.91 (s, 1H), 7.86 (d, J = 8.8 Hz, 2H), 7.09 (d, J = 8.8 Hz, 2H), 4.78 (d, J = 2.4 Hz, 2H), 2.57 (t, J = 2.4 Hz, 1H). ^{13}C NMR (101 MHz, $CDCl_3$) δ 190.77, 162.38, 131.90, 130.62, 115.19, 77.55, 76.37, 55.96.

BDP-green alkyne (**6**)



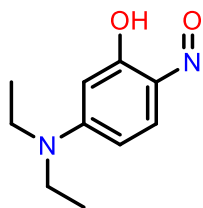
5 (500 mg, 3.12 mmol) and 2,4-dimethyl-3-ethyl-pyrrole (769 mg, 6.24 mmol) dissolved in 125 ml of dry DCM. The mixture was bubbled with N_2 for 30 minutes after which TFA (125 μ l, 1.5 mmol) was added and the mixture was left to stir for 2 hours. 2,3-Dichloro-5,6-dicyano-1,4-benzoquinone (DDQ, 708 mg, 3.12 mmol) was added and the mixture left to stir for 30 minutes. DIPEA (3.75 ml, excess) and $BF_3 \cdot OEt_2$ (3.8 ml, excess) were added subsequently and the mixture was left stirring overnight at room temperature. After purification on silica (2:3 EtOAc:PE) the 437 mg of **6** was isolated as a red, crystalline solid. Yield: 32%. 1H NMR (400 MHz, $CDCl_3$) δ 7.19 (d, J = 8.6 Hz, 2H), 7.08 (d, J = 8.7 Hz, 2H), 4.77 (d, J = 2.4 Hz, 2H), 2.56 (t, J = 2.4 Hz, 1H), 2.53 (d, J = 1.3 Hz, 6H), 2.30 (q, J = 7.5 Hz, 4H), 1.33 (s, 6H), 0.98 (t, J = 7.5 Hz, 6H). ^{13}C NMR (101 MHz, $CDCl_3$) δ 158.11, 153.76, 140.07, 138.54, 132.85, 131.25, 129.65, 129.01, 115.69, 78.26, 75.98, 56.19, 17.21, 14.76, 12.63, 11.96.

BDP-rotor alkyne (7)



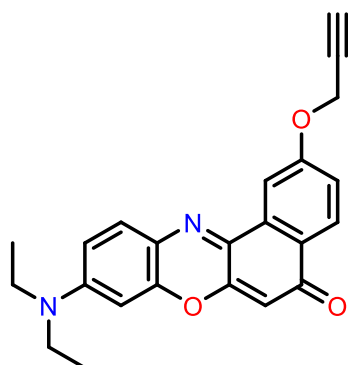
5 (500 mg, 3.12 mmol) and 2-methyl-1H-pyrrole (506 mg, 6.24 mmol) dissolved in 125 ml of dry DCM. The mixture was bubbled with N₂ for 30 minutes after which TFA (125 μ l, 1.5 mmol) was added and the mixture was left to stir for 2 hours. 2,3-Dichloro-5,6-dicyano-1,4-benzoquinone (DDQ, 708 mg, 3.12 mmol) was added and the mixture left to stir for 30 minutes. DIPEA (3.75 ml, excess) and BF₃-OEt₂ (3.8 ml, excess) were added subsequently and the mixture was left stirring overnight at room temperature. After purification on silica (2:3 EtOAc:PE) the 86 mg of **7** was isolated as a red, crystalline solid. Yield: 8%. **¹H NMR** (400 MHz, CDCl₃) δ 7.47 (d, J = 8.7 Hz, 2H), 7.08 (d, J = 8.7 Hz, 2H), 6.74 (d, J = 4.1 Hz, 2H), 6.27 (d, J = 4.2 Hz, 2H), 4.78 (d, J = 2.4 Hz, 2H), 2.65 (s, 6H), 2.58 (t, J = 2.4 Hz, 1H). **¹³C NMR** (101 MHz, CDCl₃) δ 159.14, 157.20, 142.30, 134.51, 131.96, 130.27, 127.43, 119.26, 114.62, 78.06, 76.08, 55.92, 14.88.

5-(diethylamino)-2-nitrosophenol (8)



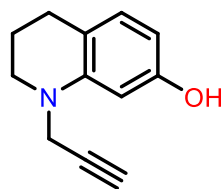
3-diethylaminophenol (8.7 g, 52.7 mmol) was dissolved in 30 ml concentrated HCl + 10 ml H₂O. The solution was cooled to 0 °C after which NaNO₂ (4.36 g, 63 mmol) dissolved in 30 ml H₂O was added dropwise. The mixture was left stirring for 1h, filtered and the residue washed with a saturated sodium acetate solution. The residue was recrystallized from acetone, yielding 1.07g of **8**. Yield: 16%. **¹H NMR** (400 MHz, DMSO) δ 7.31 (d, J = 9.9 Hz, 1H), 6.88 (dd, J = 10.0, 2.6 Hz, 1H), 5.74 (d, J = 2.6 Hz, 1H), 3.59 (q, J = 7.1 Hz, 4H), 1.18 (t, J = 7.1 Hz, 6H). **¹³C NMR** (101 MHz, DMSO) δ 169.20, 157.56, 149.71, 134.96, 115.72, 95.60, 46.07, 13.64

NR-alkyne (9)



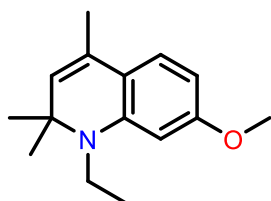
8 (292 mg, 1.27 mmol) and 1,6-dihydroxynaphthalene (204 mg, 1.27 mmol) were dissolved in 10 ml DMF and refluxed at 155 °C for 4 hour. The mixture was cooled to 110 °C after which K₂CO₃ (675 mg, 5.08 mmol) was added followed by propargyl bromide (0.55 ml from a 80% solution in toluene, 5.08 mmol) and left stirring for 1 hour at 110 °C. The mixture was cooled to room temperature and diluted with Et₂O (25 ml) and brine (25 ml). The aqueous layer was washed with 3x25 ml Et₂O and the organic layers were combined, concentrated and purified on silica (2:1 hexane:EtOAc, 5% TEA) yielding 60 mg of **9**. Yield: 13%. **¹H NMR** (400 MHz, CDCl₃) δ 8.25 (d, J = 8.8 Hz, 1H), 8.14 (d, J = 2.6 Hz, 1H), 7.56 (d, J = 9.1 Hz, 1H), 7.23 (d, J = 2.6 Hz, 1H), 6.66 (dd, J = 9.0, 2.7 Hz, 1H), 6.47 (d, J = 2.7 Hz, 1H), 6.33 (s, 1H), 4.90 (d, J = 2.4 Hz, 2H), 3.47 (qd, J = 7.1, 4.3 Hz, 10H), 2.58 (t, J = 2.4 Hz, 1H), 1.26 (td, J = 7.1, 5.7 Hz, 18H).

1-(prop-2-yn-1-yl)-1,2,3,4-tetrahydroquinolin-7-ol (10)



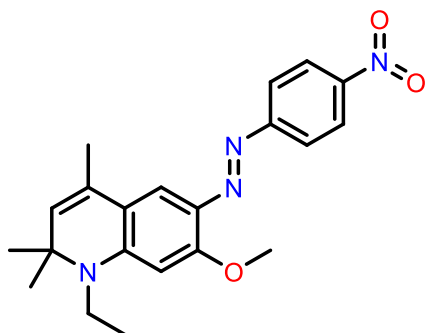
7-hydroxy-1,2,3,4-tetrahydroquinoline (1g, 6.67 mmol) and K₂CO₃ (1.1 g, 8 mmol) were dissolved in 8.5 ml of dry DMF. Propargyl bromide (1.5 ml from a 80% solution in toluene, 10 mmol) was added and the mixture left to stir for 1.5 hours at 65 °C. The mixture was cooled to room temperature, EtOAc (100 ml) and H₂O (20 ml) were added. The aqueous layer was washed with 3x20 ml EtOAc. The organic layers were combined, concentrated and purified on silica (1:4 EtOAc:hexane) yielding 761 mg of **10**. Yield: 61%. **¹H NMR** (400 MHz, CDCl₃) δ 6.82 (d, J = 8.0 Hz, 1H), 6.24 (d, J = 2.4 Hz, 1H), 6.15 (dd, J = 8.0, 2.4 Hz, 1H), 4.55 (s, 1H), 3.97 (d, J = 2.4 Hz, 2H), 3.34 – 3.18 (m, 2H), 2.69 (t, J = 6.5 Hz, 2H), 2.16 (t, J = 2.4 Hz, 1H), 2.02 – 1.93 (m, 2H). **¹³C NMR** (101 MHz, CDCl₃) δ 154.73, 145.58, 129.78, 116.47, 104.12, 99.30, 79.48, 71.75, 49.12, 40.76, 26.91, 22.54.

1-ethyl-7-methoxy-2,2,4-trimethyl-1,2-dihydroquinoline (11)



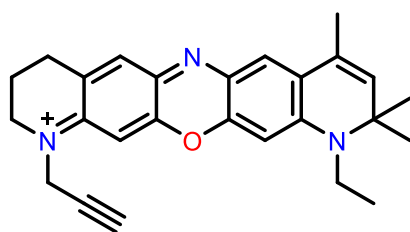
7-methoxy-2,2,4-trimethyl-1,2-dihydroquinoline (2 g, 9.8 mmol) and K_2CO_3 (2.12 g, 15.4 mmol) were added to 35 ml MeCN. Iodoethane (2 ml, 24.8 mmol) was added and the mixture was left stirring overnight at 90 °C. The mixture was filtered, concentrated and purified on silica (1:19 EtOAc:cyclohexane) yielding 850 mg of **11**. Yield: 37%. 1H NMR (400 MHz, $CDCl_3$) δ 6.96 (d, J = 8.3 Hz, 1H), 6.14 (dd, J = 8.3, 2.4 Hz, 1H), 6.08 (d, J = 2.4 Hz, 1H), 5.10 (q, J = 1.4 Hz, 1H), 3.79 (s, 3H), 3.30 (d, J = 7.1 Hz, 2H), 1.94 (d, J = 1.4 Hz, 3H), 1.30 (s, 6H), 1.20 (t, J = 7.0 Hz, 3H). ^{13}C NMR (101 MHz, $CDCl_3$) δ 160.53, 144.98, 127.35, 126.99, 124.44, 116.60, 98.76, 97.51, 56.89, 55.09, 38.19, 18.76, 14.25.

(E)-1-ethyl-7-methoxy-2,2,4-trimethyl-6-((4-nitrophenyl)diazenyl)-1,2-dihydroquinoline (12)



11 (200 mg, 0.86 mmol) was dissolved in 8 ml MeOH. A suspension of 4-nitrobenzenediazonium tetrafluoroborate (215 mg, 0.91 mmol) in 1 ml of a 10 % H_2SO_4 in H_2O was added dropwise, the resulting solution was stirred for 1 hour and then cooled on ice before adding 0.16 ml of a 30% NH_4OH solution. The precipitate was isolated, washed with 300 ml of H_2O , and then purified on silica (1:4 EtOAc:cyclohexane) yielding 286 mg of **12**. Yield: 87%. 1H NMR (400 MHz, $CDCl_3$) δ 8.29 (d, J = 9.0 Hz, 2H), 7.87 (d, J = 9.0 Hz, 2H), 7.66 (s, 1H), 6.07 (s, 1H), 5.27 (d, J = 1.5 Hz, 1H), 4.04 (s, 3H), 3.51 (q, J = 7.1 Hz, 2H), 2.02 (d, J = 1.4 Hz, 3H), 1.41 (s, 6H), 1.33 (t, J = 7.0 Hz, 3H). ^{13}C NMR (101 MHz, $CDCl_3$) δ 161.20, 157.97, 150.28, 146.76, 133.44, 128.54, 127.04, 124.83, 122.51, 116.48, 112.50, 93.24, 77.48, 77.16, 76.84, 58.78, 56.46, 39.18, 29.56, 27.07, 18.92, 13.98, 0.14.

Oxazine alkyne (**13**)



10 (24.5 mg, 0.13 mmol) and **12** (50 mg, 0.13 mmol) were dissolved in an aqueous 1.5% HCl solution. The solution was heated to 80 °C for 4 hours, cooled and concentrated followed by purification on silica (1:19 MeOH:CHCl₃) yielding 42 mg of **13** which was not pure by NMR. ¹H NMR (400 MHz, CDCl₃) δ 7.47 (s, 1H), 7.36 (s, 1H), 7.28 (s, 1H), 6.47 (s, 1H), 5.53 (d, J = 1.5 Hz, 1H), 4.27 – 4.18 (m, 1H), 3.82 (q, J = 5.7 Hz, 2H), 3.74 (s, 2H), 3.73 – 3.66 (m, 3H), 3.25 (d, J = 7.5 Hz, 3H), 2.88 (t, J = 6.3 Hz, 3H), 2.29 (s, 2H), 2.14 – 2.07 (m, 3H), 2.06 (s, 3H), 2.04 – 1.95 (m, 4H), 1.52 (s, 6H).

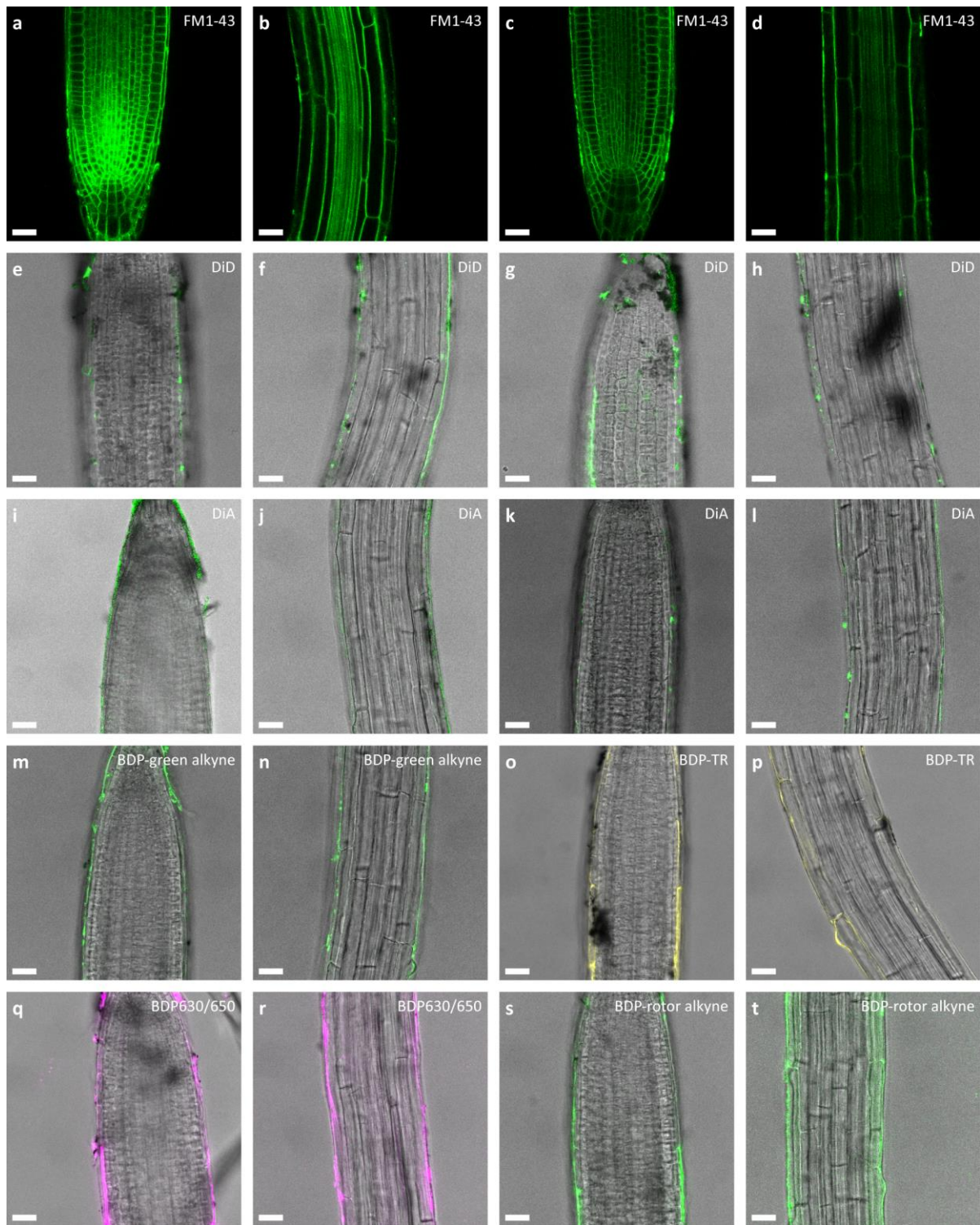


Fig. S1. Staining of Arabidopsis with commonly used mammalian membrane probes and LipoTag dye precursors. **a-d**, Staining of different regions of Arabidopsis roots with 10 μM (**a,b**) and 1 μM (**c,d**) FM1-43. **e-h**, Staining of different regions of Arabidopsis roots with 10 μM (**e,f**) and 1 μM (**g,h**) DiD. **i-l**, Staining of different regions of Arabidopsis roots with 10 μM (**i,j**) and 1 μM (**k,l**) DiA. **m-n**, Staining of Arabidopsis root with 1 μM LipoTag-Green precursor BDP-alkyne green (6). **o-p**, Staining of Arabidopsis root with 1 μM LipoTag-Orange precursor BDP-TR alkyne. **q-r**, Staining of Arabidopsis root with 1 μM LipoTag-Red precursor BDP630/650 alkyne. **s-t**, Staining of Arabidopsis root with 1 μM LipoTag-BDP precursor BDP-alkyne green (6). **m-n**, Staining of Arabidopsis root with 1 μM LipoTag-Green precursor BDP-rotor alkyne (7). Scale bars represent 25 μm .

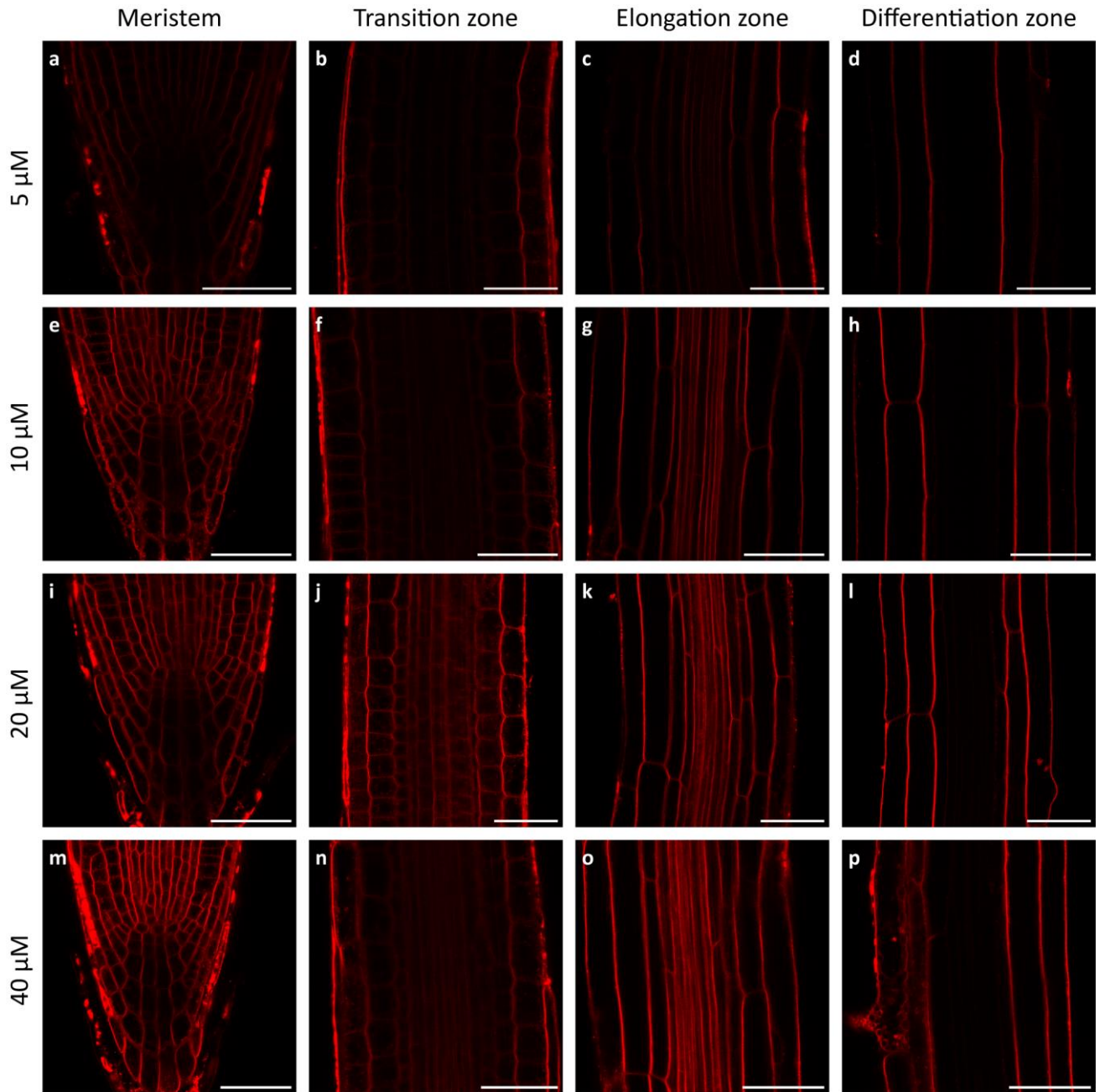


Fig. S2. Concentration range FM4-64 in different Arabidopsis root zones.

Concentration range with FM4-64 for different root tissues with 5 μM in 0.5x MS (**a-d**), 10 μM in 0.5x MS (**e-h**), 20 μM in 0.5x MS (**i-l**), and 40 μM in 0.5x MS (**m-p**) for 20 minutes. All measurements were performed and processed the same way. Scale bar represents 40 μm.

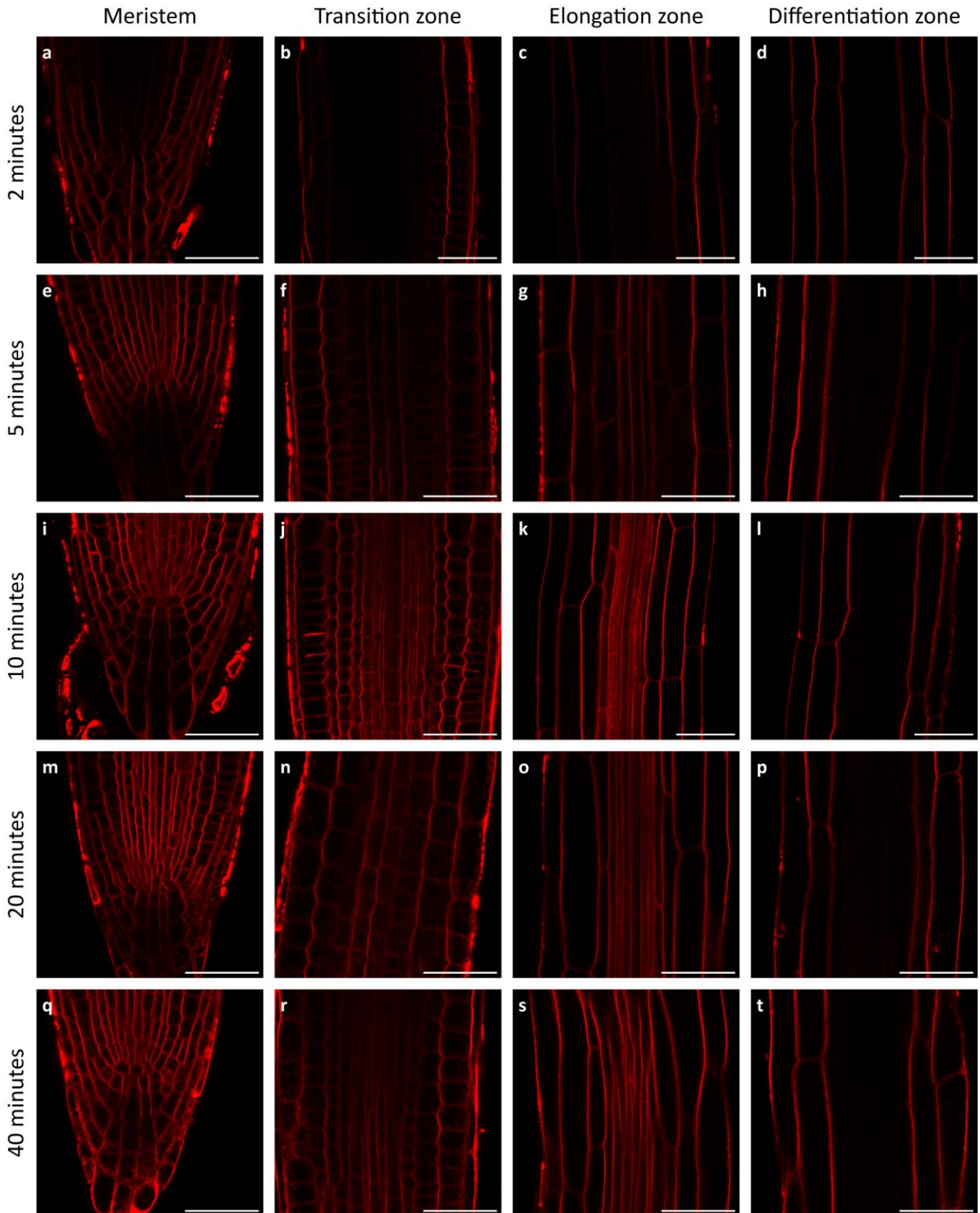


Fig. S3. Penetration depth of FM4-64 in different tissues over time.

Time series for FM4-64 at 20 μ M in 0.5x MS for different root tissues at time 2 minutes (**a-d**), 5 minutes (**d-h**), 10 minutes (**i-l**), 20 minutes (**m-p**), 40 minutes (**q-t**). All measurements were performed and processed the same way. Scale bar represents 40 μ m.

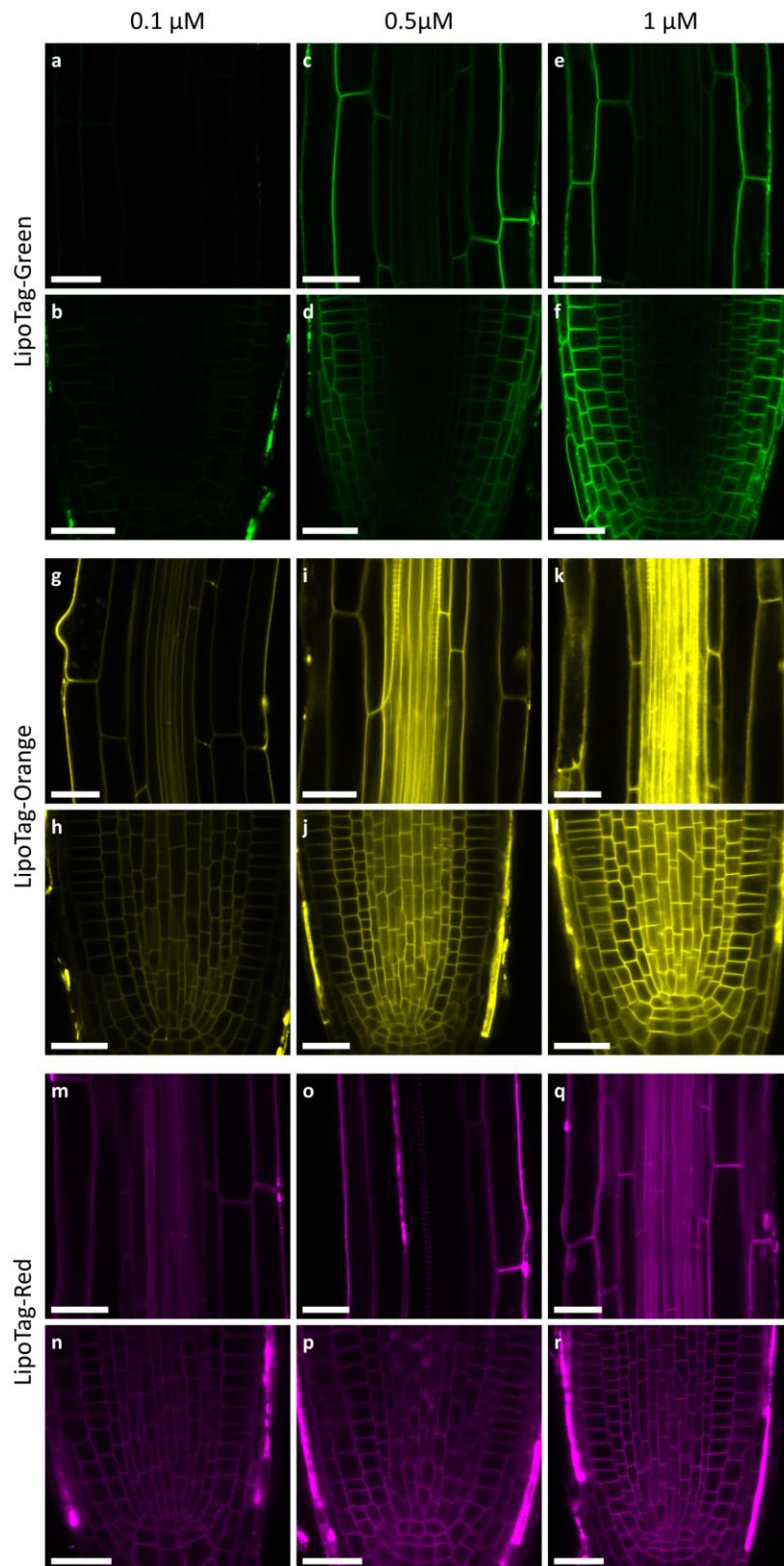


Fig. S4. Effect of staining concentration of non-functional LipoTag probes on tissue penetration after 30 minutes. **a-f**, Staining of LipoTag-Green in the elongation zone (**a,c,e**) and the root tip (**b,d,f**) after 30 minutes of incubation. **g-l**, Staining of LipoTag-Orange in the elongation zone (**g,i,k**) and the root tip (**h,j,l**) after 30 minutes of incubation. **m-r**, Staining of LipoTag-Red in the elongation zone (**m,o,q**) and the root tip (**n,p,r**) after 30 minutes of incubation. All measurements were performed and processed the same way. Scale bar represents 25 μm.

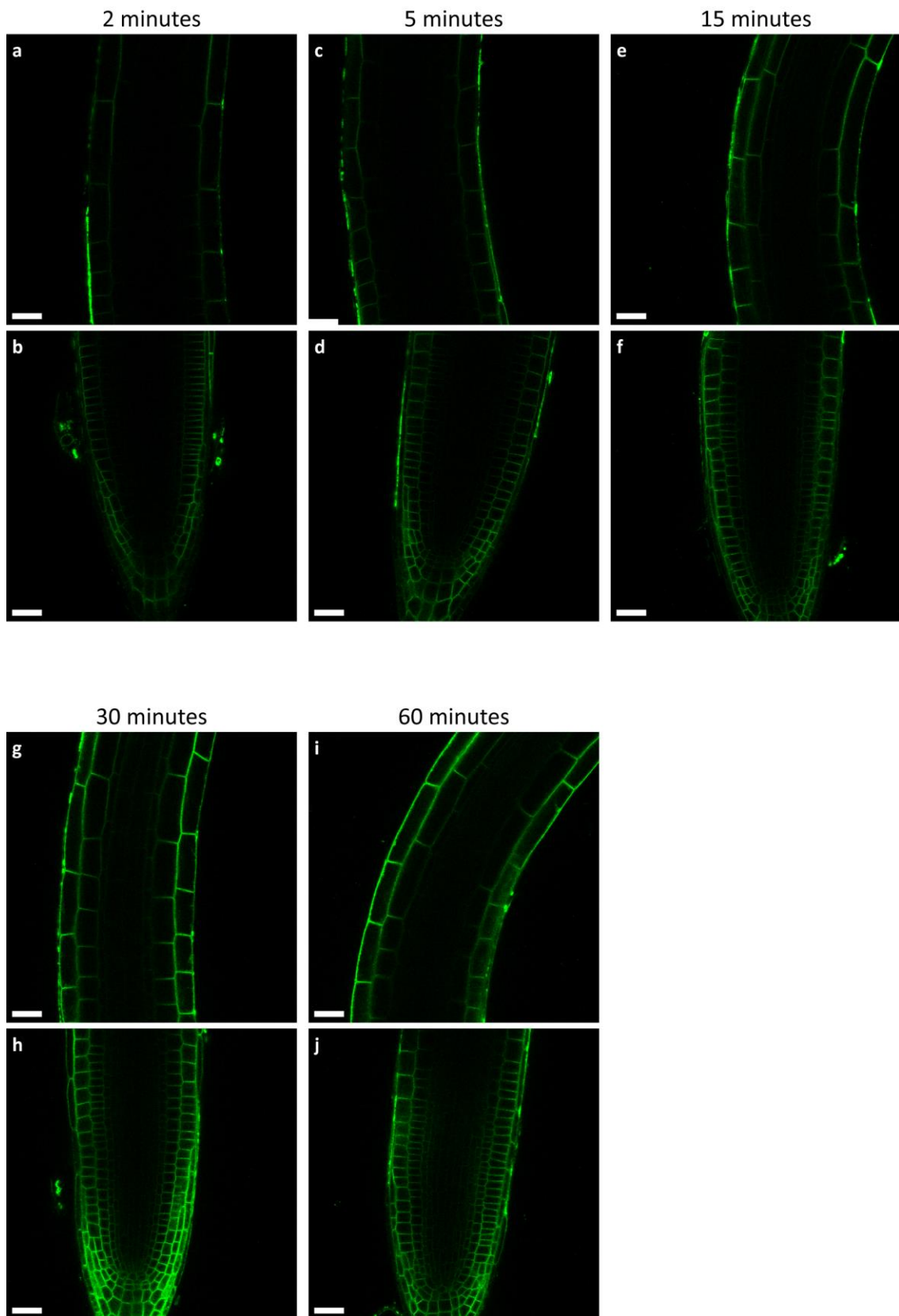


Fig. S5. Staining kinetics of LipoTag-Green in the root tip and elongation zone.

Images of Arabidopsis root stained with 0.5 μM LipoTag-Green after 2 minutes (a,b), 5 minutes (c,d), 15 minutes (e,f), 30 minutes (g,h) and 60 minutes (i,j). All measurements were performed and processed the same way. Scale bar represents 25 μm .

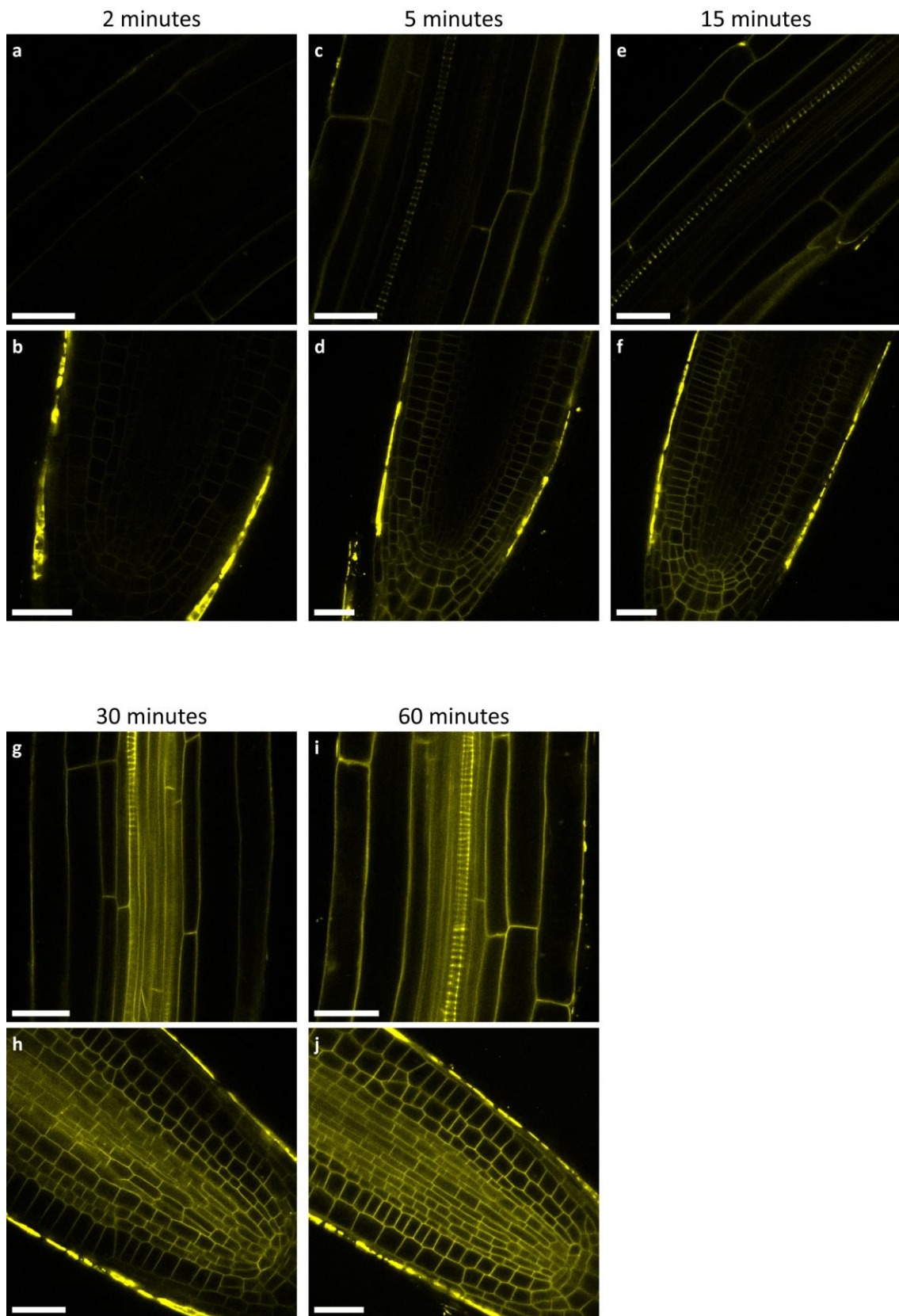


Fig. S6. Staining kinetics of LipoTag-Orange in the root tip and elongation zone.

Images of Arabidopsis root stained with 0.5 μM LipoTag-Orange after 2 minutes (a,b), 5 minutes (c,d), 15 minutes (e,f), 30 minutes (g,h) and 60 minutes (i,j). All measurements were performed and processed the same way. Scale bar represents 25 μm .

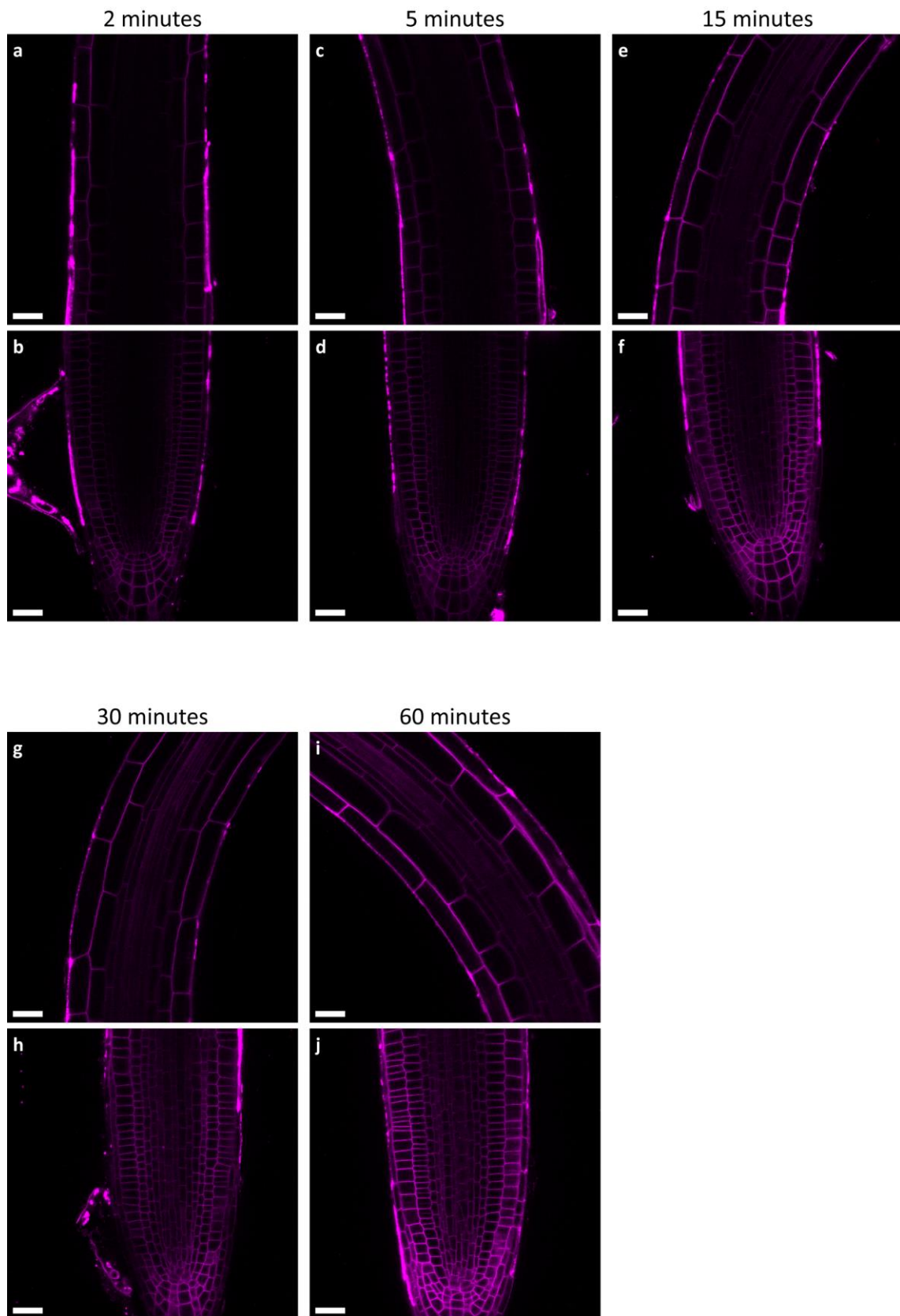


Fig. S7. Staining kinetics of LipoTag-Red in the root tip and elongation zone.

Images of Arabidopsis root stained with 0.5 μM LipoTag-Red after 2 minutes (**a,b**), 5 minutes (**c,d**), 15 minutes (**e,f**), 30 minutes (**g,h**) and 60 minutes (**i,j**). All measurements were performed and processed the same way. Scale bar represents 25 μm.

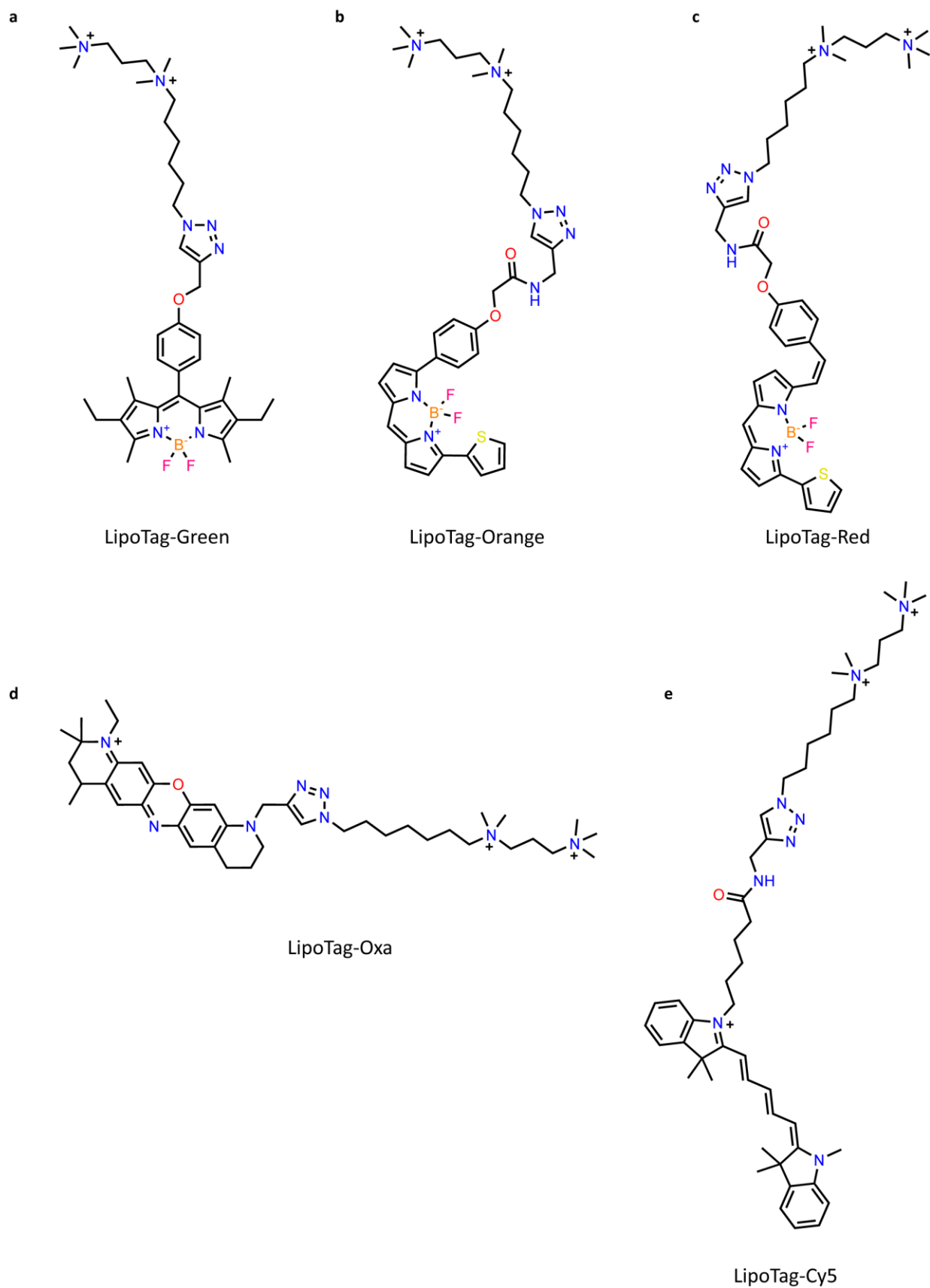


Fig. S8. Chemical structures of non-functional LipoTag probes.

Chemical structure of LipoTag-Green (a), LipoTag-Orange (b), LipoTag-Red (c), LipoTag-Oxa (d) and LipoTag-Cy5 (e)

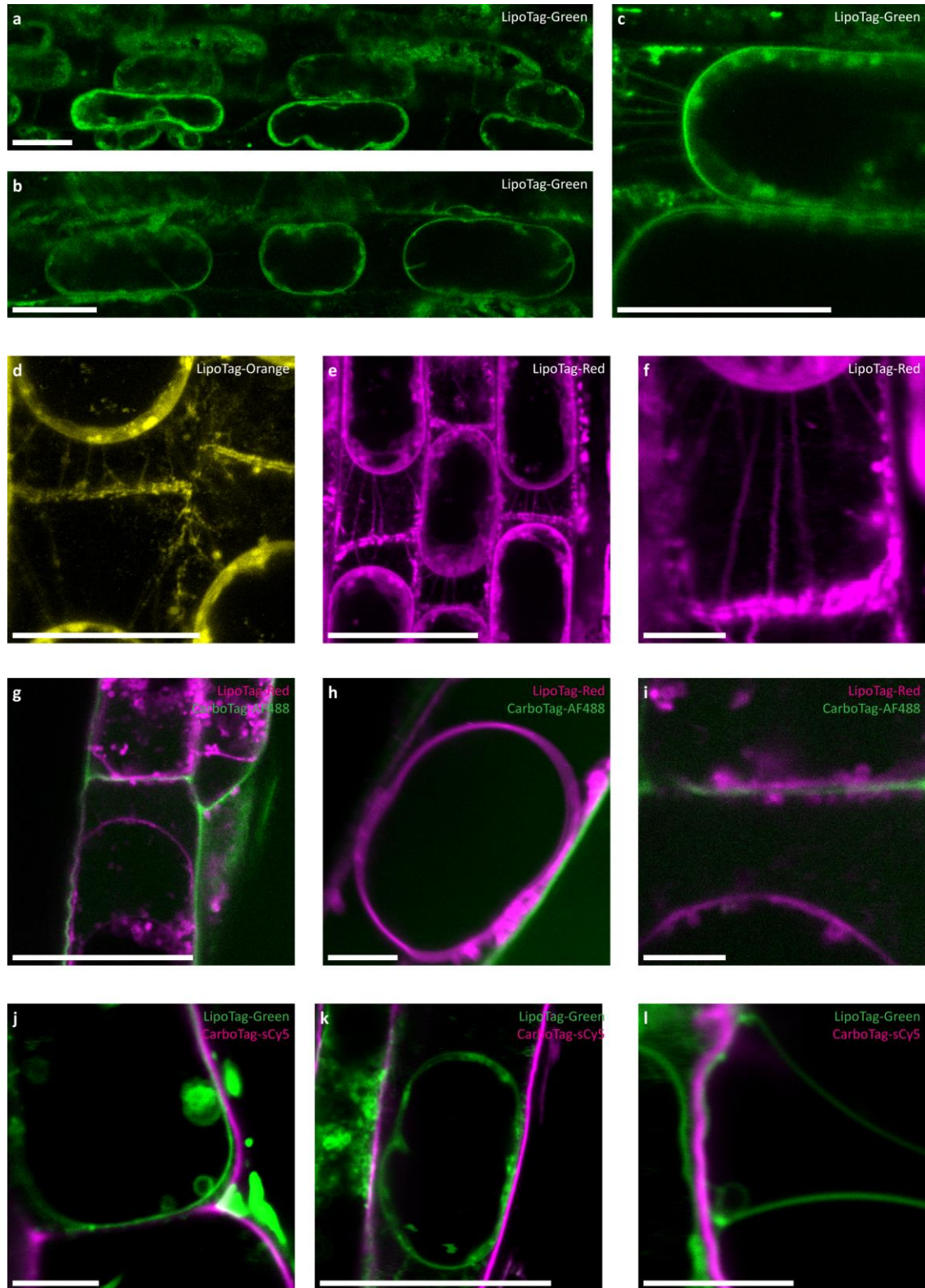


Fig. S9. Plasmolysis of LipoTag stained Arabidopsis roots.

Arabidopsis roots stained with LipoTag-Green (**a-c**), LipoTag-Orange (**b**) and LipoTag-Red (**e-f**) after gradual plasmolysis with 0.3 M mannitol followed by 0.5 M mannitol. Besides the retracted membrane Hechtian strands and the Hechtian reticulum are visible. To confirm membrane localization CarboTag-AF488 (green) and CarboTag-sCy5 (magenta) were used to co-stain the cell wall during plasmolysis with LipoTag-Red (magenta) (**g-i**) and LipoTag-Green (green) (**j-l**) respectively. Scale bars represent 5 μm for **f**, **h**, **i**, **j** and **l**, all others represent 25 μm .

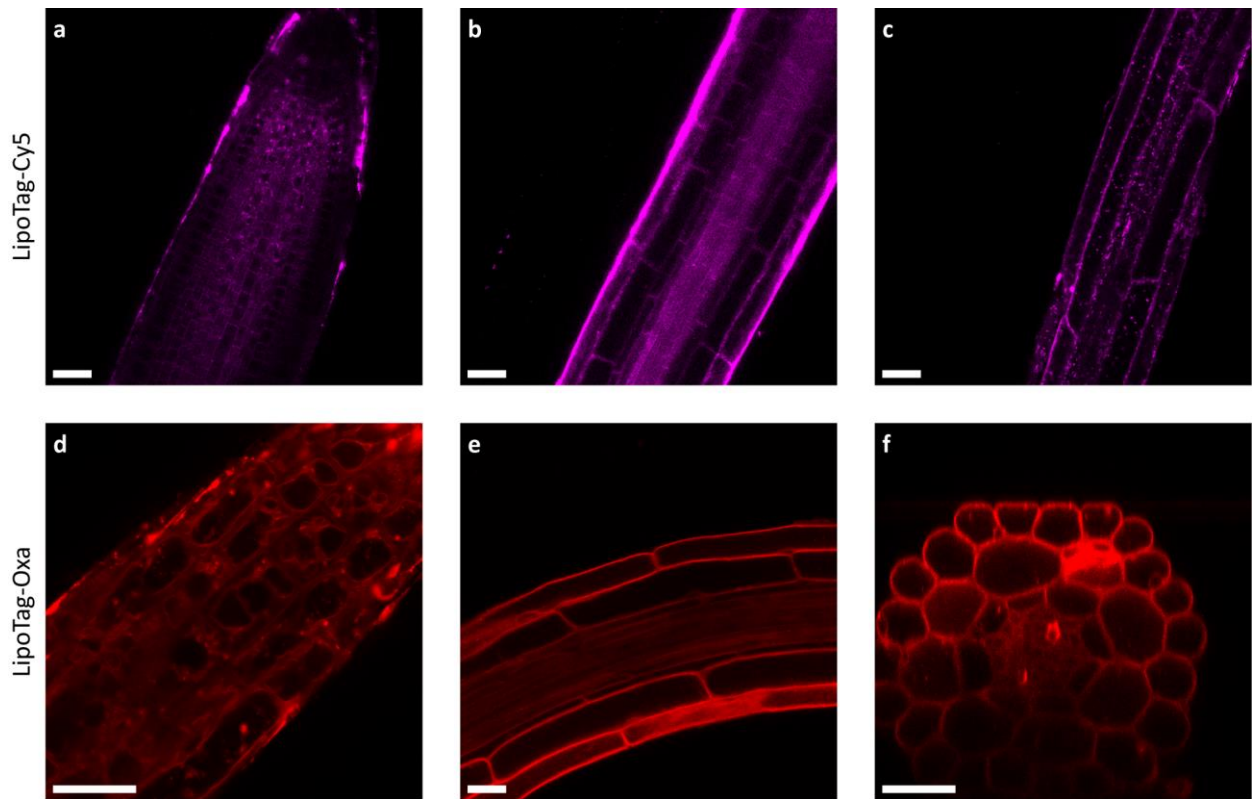
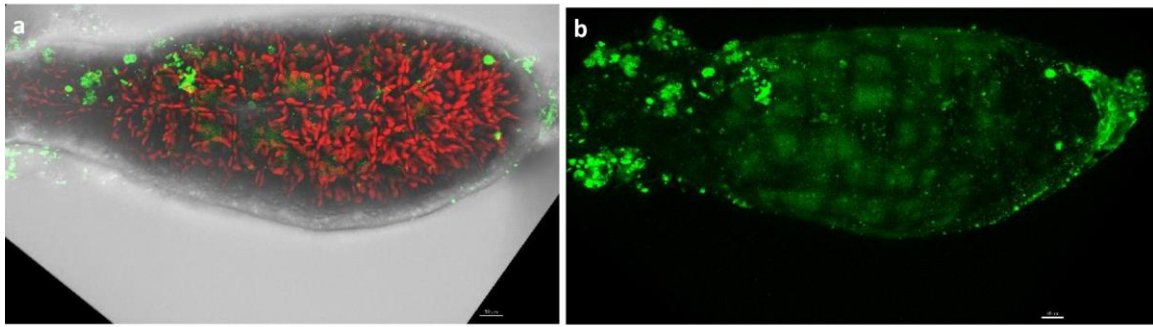


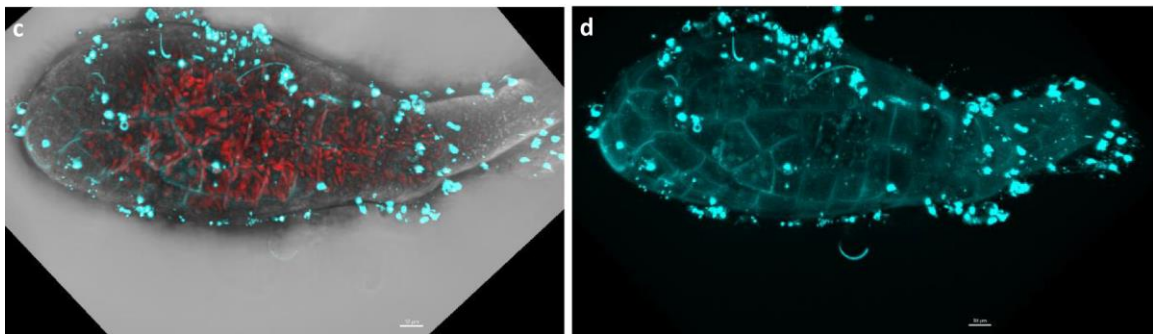
Fig. S10. Staining of Arabidopsis roots with LipoTag-Cy5 and LipoTag-Oxa.

Staining of Arabidopsis roots with 1 μM LipoTag-Cy5 (**a-c**) and 1 μM LipoTag-Oxa (**d**) and 0.1 μM LipoTag-Oxa (**e-f**). **f** is a xzy projection. Scale bars represent 25 μm .

LipoTag-Green



LipoTag-Orange



LipoTag-Red

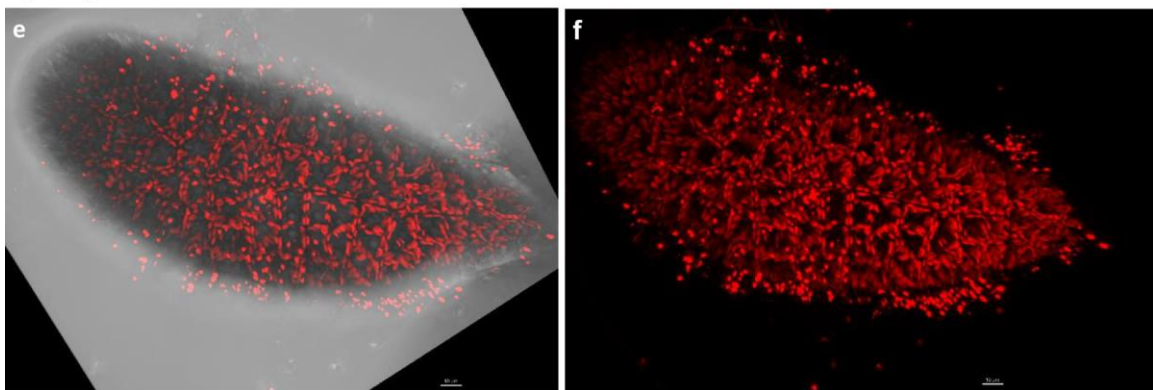
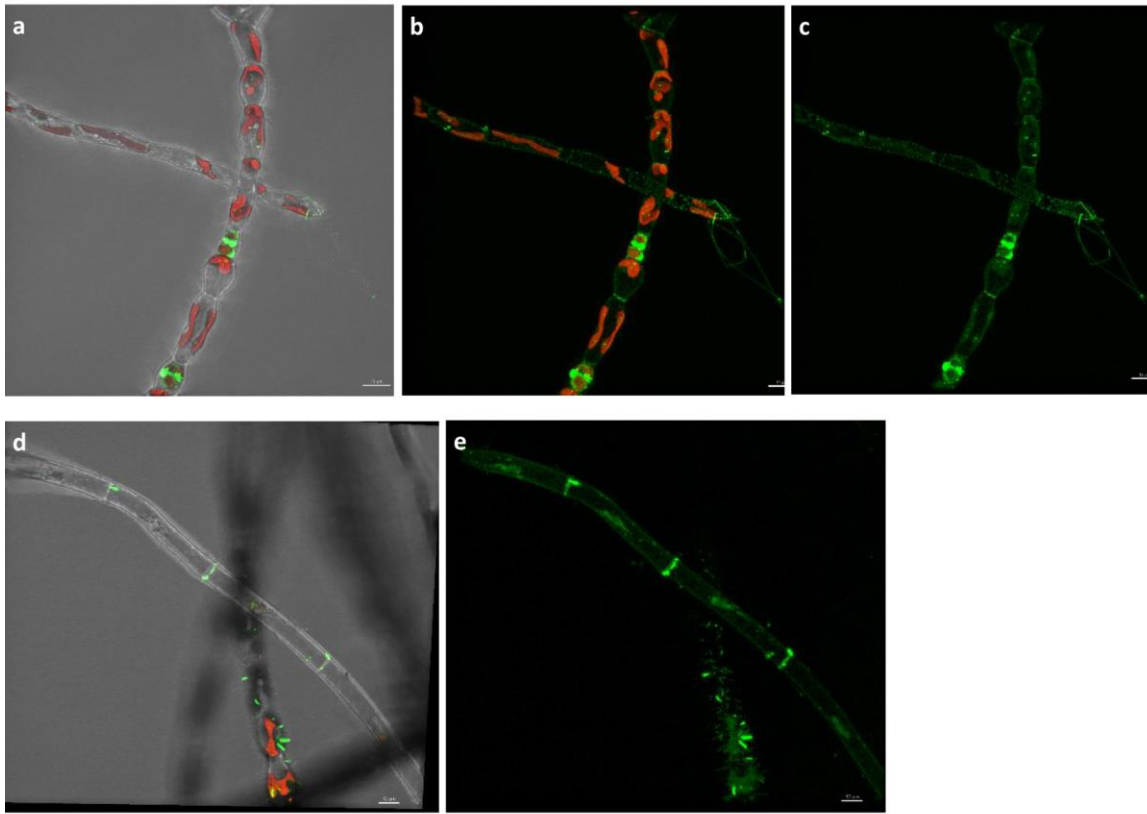


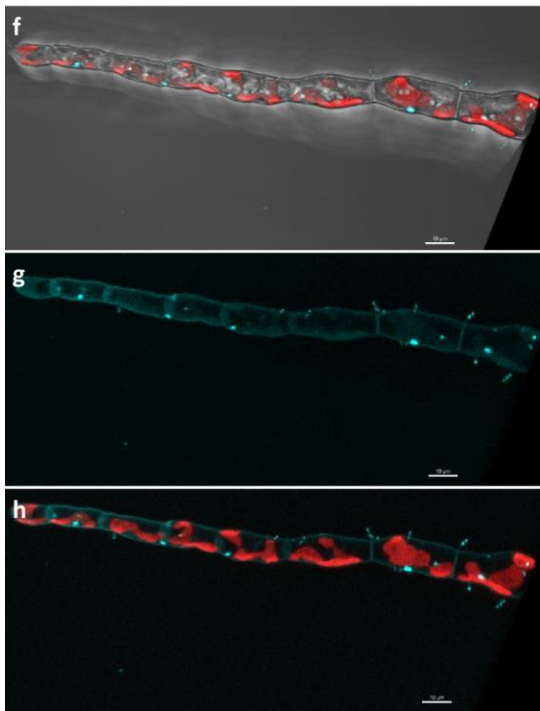
Fig. S11. Staining of *F. serratus* with LipoTag probes.

Images of *F. serratus* stained with LipoTag-Green (green) (**a-b**) with the brightfield overlay shown in **a**, LipoTag-Orange (cyan) (**c-d**) with the brightfield overlay shown in **c** and LipoTag-Red (red) (**e-f**) with the brightfield overlay shown in **e**. Chlorophyll autofluorescence is shown in red, scale bars represent 10 μm .

LipoTag-Green



LipoTag-Orange



LipoTag-Red

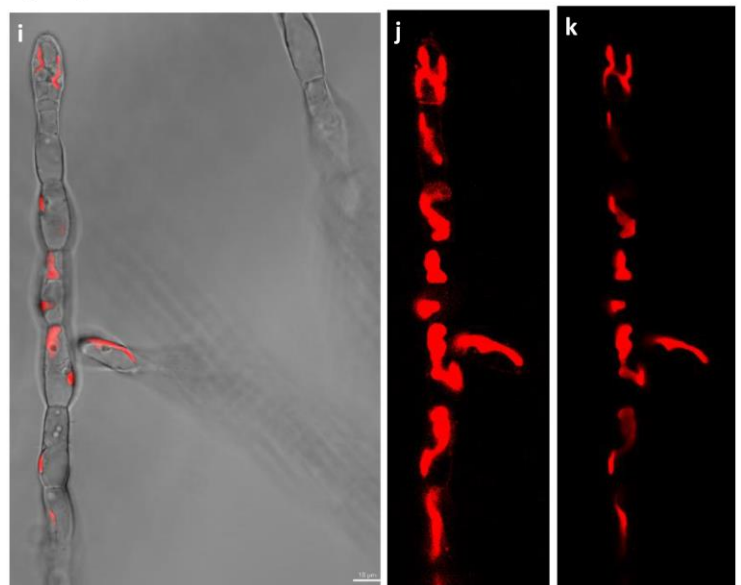
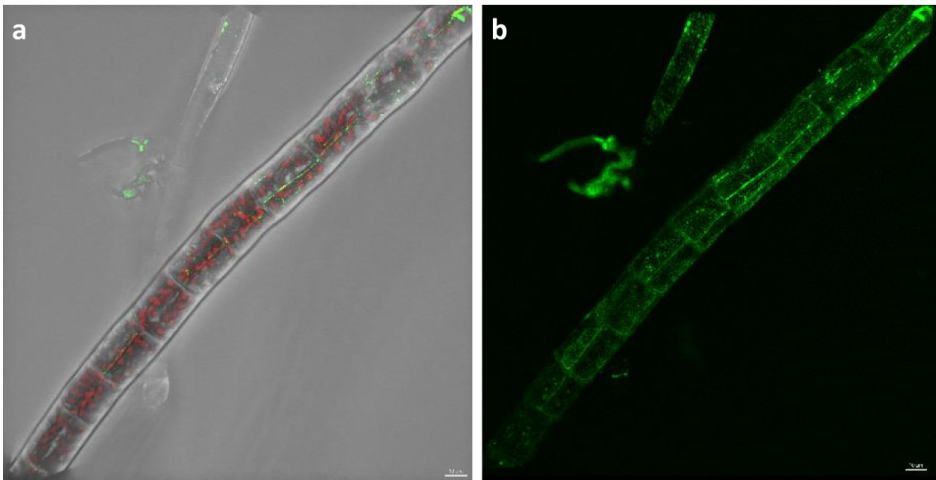


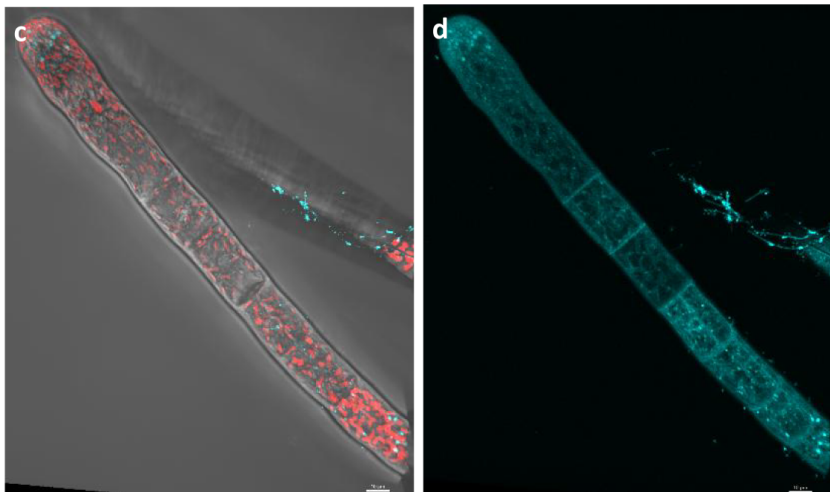
Fig. S12. Staining of *Ectocarpus* sp. with LipoTag probes.

Images of *Ectocarpus* sp. stained with LipoTag-Green (green) (a-e) with the brightfield overlay shown in a and d, LipoTag-Orange (cyan) (f-h) with the brightfield overlay shown in f and LipoTag-Red (red) (i-k) with the brightfield overlay shown in i. Chlorophyll autofluorescence is shown in red, scale bars represent 10 μm.

LipoTag-Green



LipoTag-Orange



LipoTag-Red

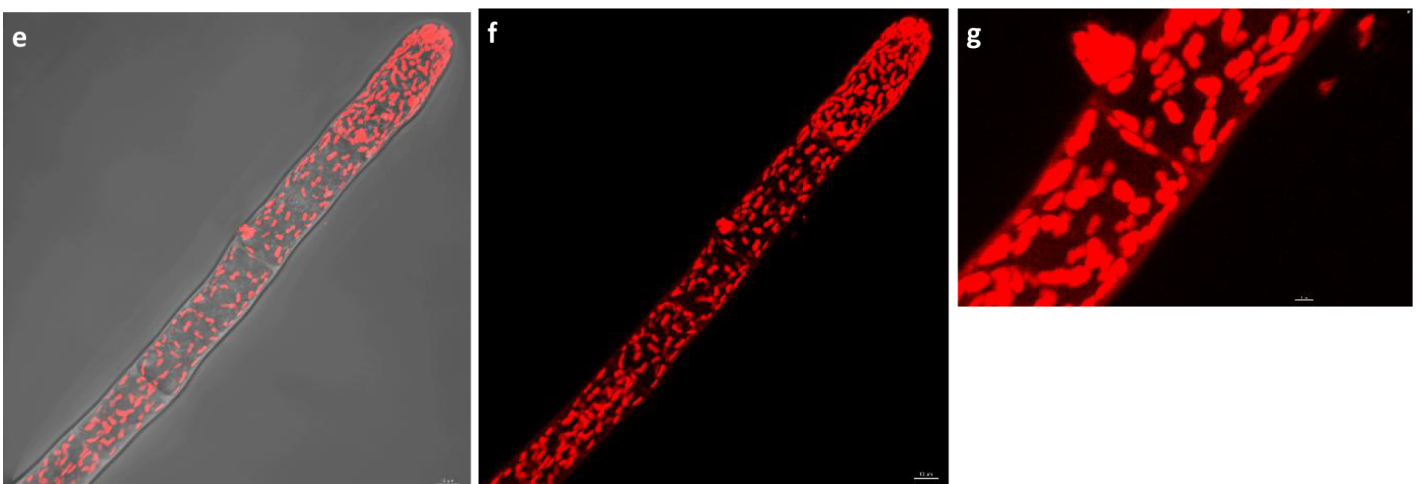
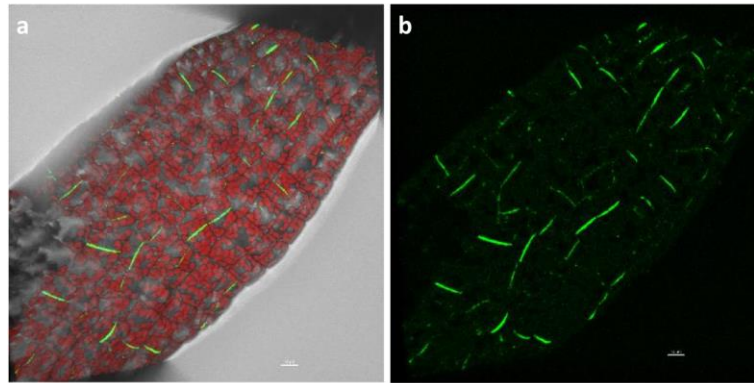


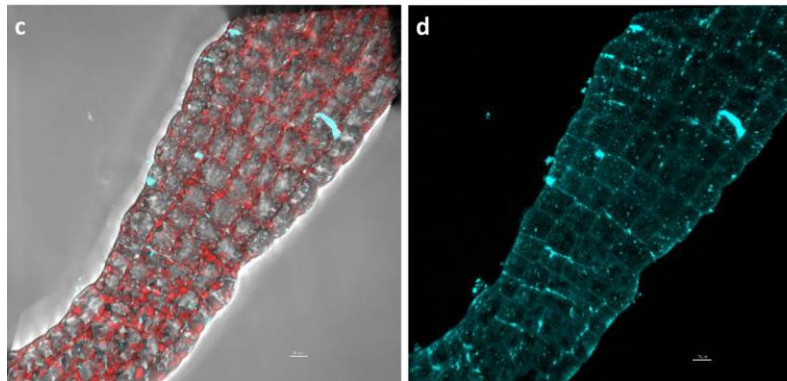
Fig. S13. Staining of *S. rigidula* with LipoTag probes.

Images of *S. rigidula* stained with LipoTag-Green (green) (a-b) with the brightfield overlay shown in a, LipoTag-Orange (cyan) (c-d) with the brightfield overlay shown in c and LipoTag-Red (red) (e-g) with the brightfield overlay shown in e. Chlorophyll autofluorescence is shown in red, scale bars represent 10 μm .

LipoTag-Green



LipoTag-Orange



LipoTag-Red

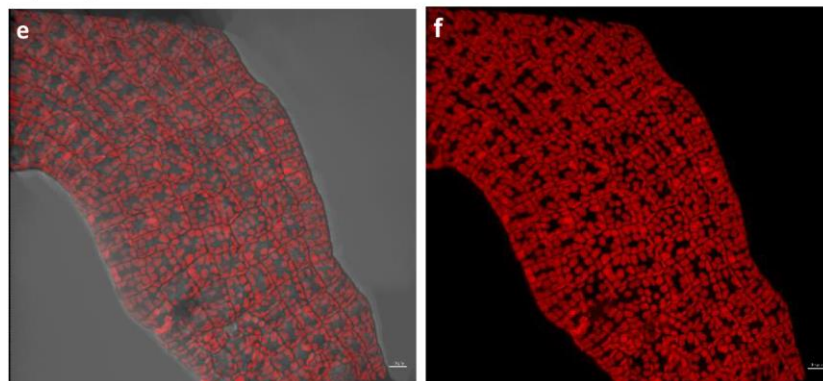


Fig. S14. Staining of *S. latissima* with LipoTag probes.

Images of *S. latissima* stained with LipoTag-Green (green) (a-b) with the brightfield overlay shown in a, LipoTag-Orange (cyan) (c-d) with the brightfield overlay shown in c and LipoTag-Red (red) (e-f) with the brightfield overlay shown in e. Chlorophyll autofluorescence is shown in red, scale bars represent 10 μm .

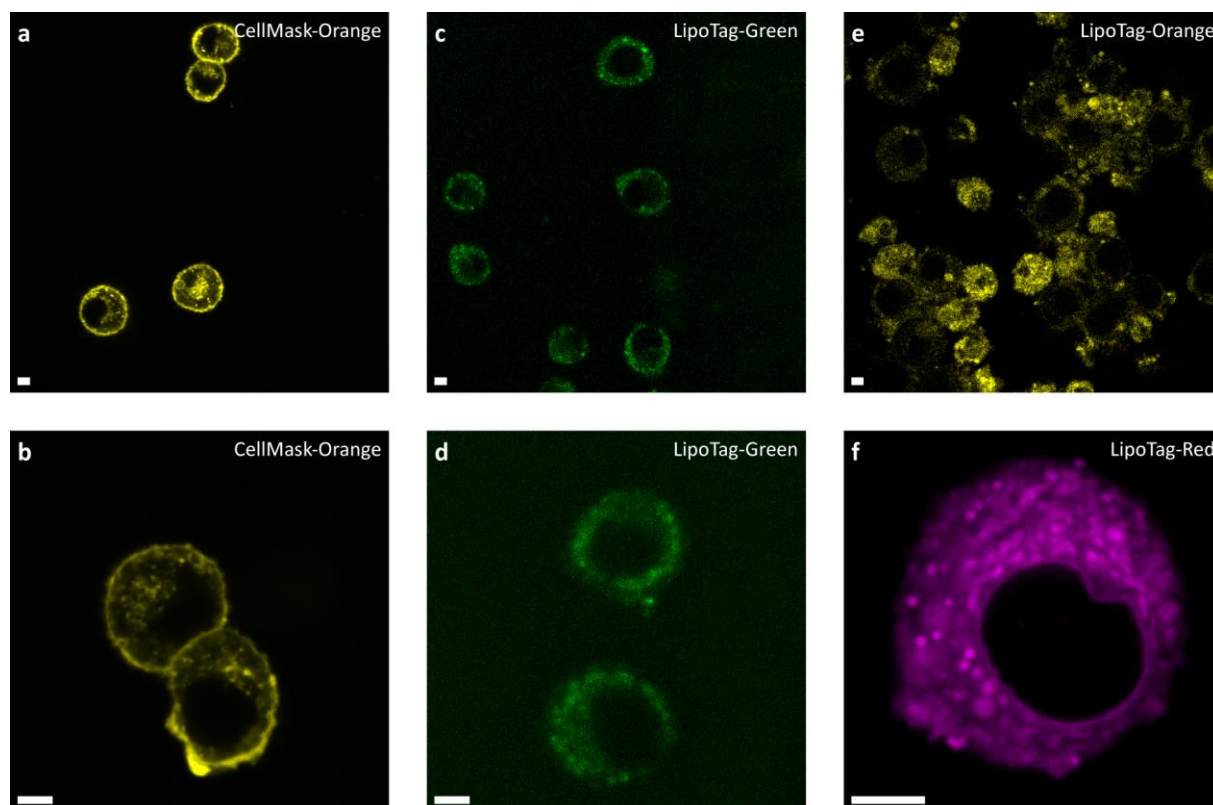


Fig. S15. Staining of Murine macrophage cells with LipoTag dyes.

Images of Murine cells stained with Cellmask-Orange (**a-b**), LipoTag-Green (**c-d**), LipoTag-Orange (**e**) and LipoTag-Red (**f**). Scale bars represent 5 μm.

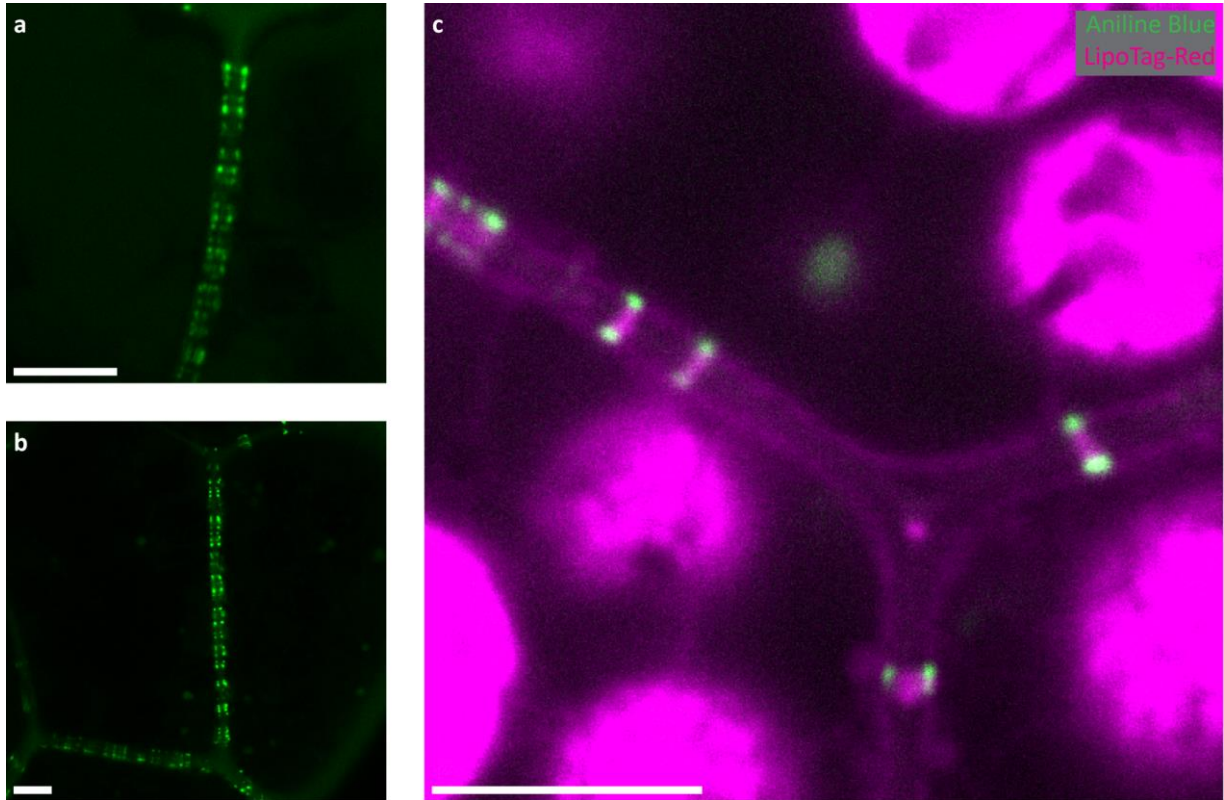


Fig. S16. Staining of plasmodesmata in *Marchantia* gemmae.

Staining of plasmodesmata in *Marchantia* gemmae with Aniline Blue (**a-b**) and gemmae co-stained with Aniline Blue (green) and LipoTag-Red (magenta) (**c**). Autofluorescence of chlorophyll is visible together with the outline of cell membranes and the plasmodesmata membrane. Scale bars represent 5 μm .

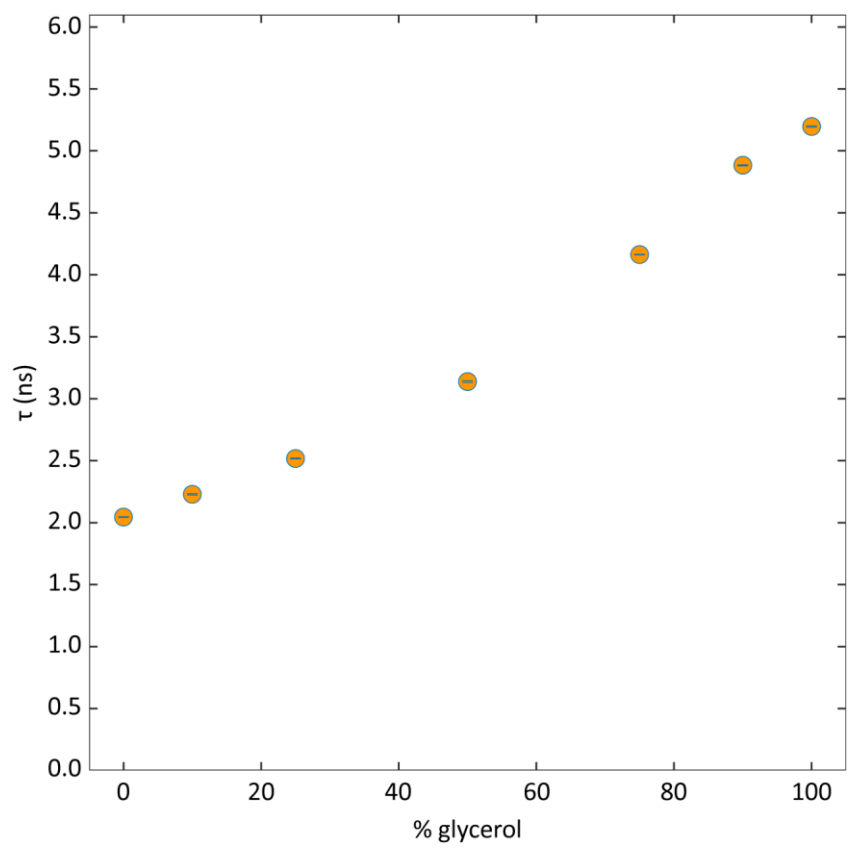


Fig. S17. Calibration of LipoTag-BDP.

Fluorescence lifetime of LipoTag-BDP in mixtures with varying glycerol concentration. All measurements were repeated 5 times, error bars fall within the point size.

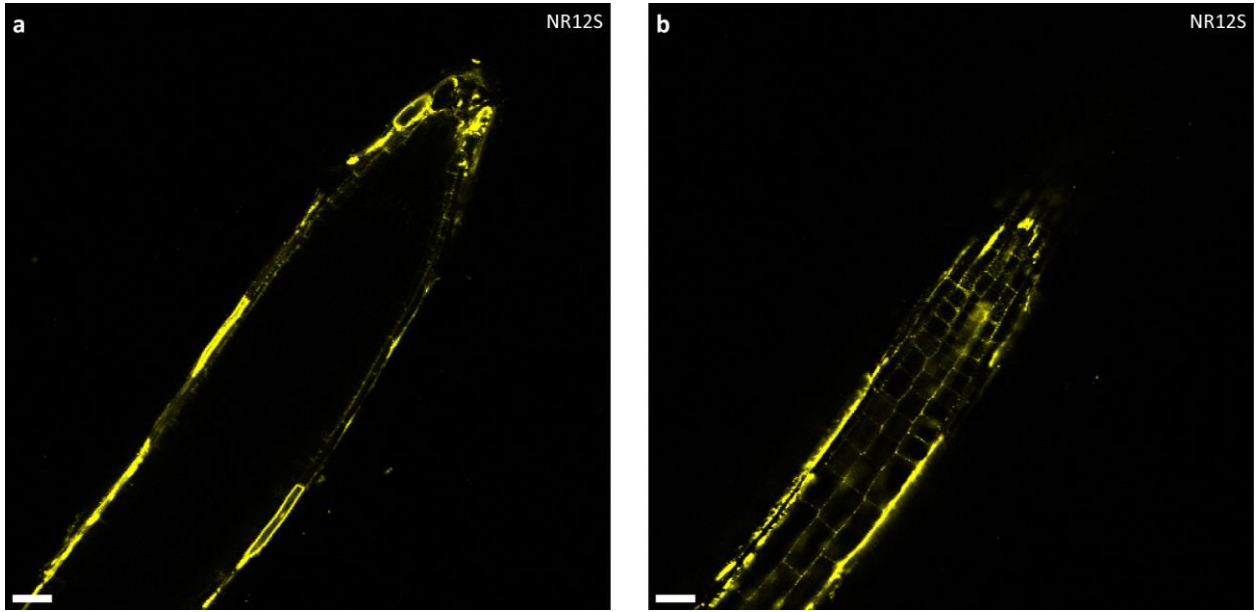


Fig. S18. Staining of Arabidopsis root with NR12S.

Staining of Arabidopsis root with 10 μM NR12S for 1 hour. Scale bars represent 25 μm .

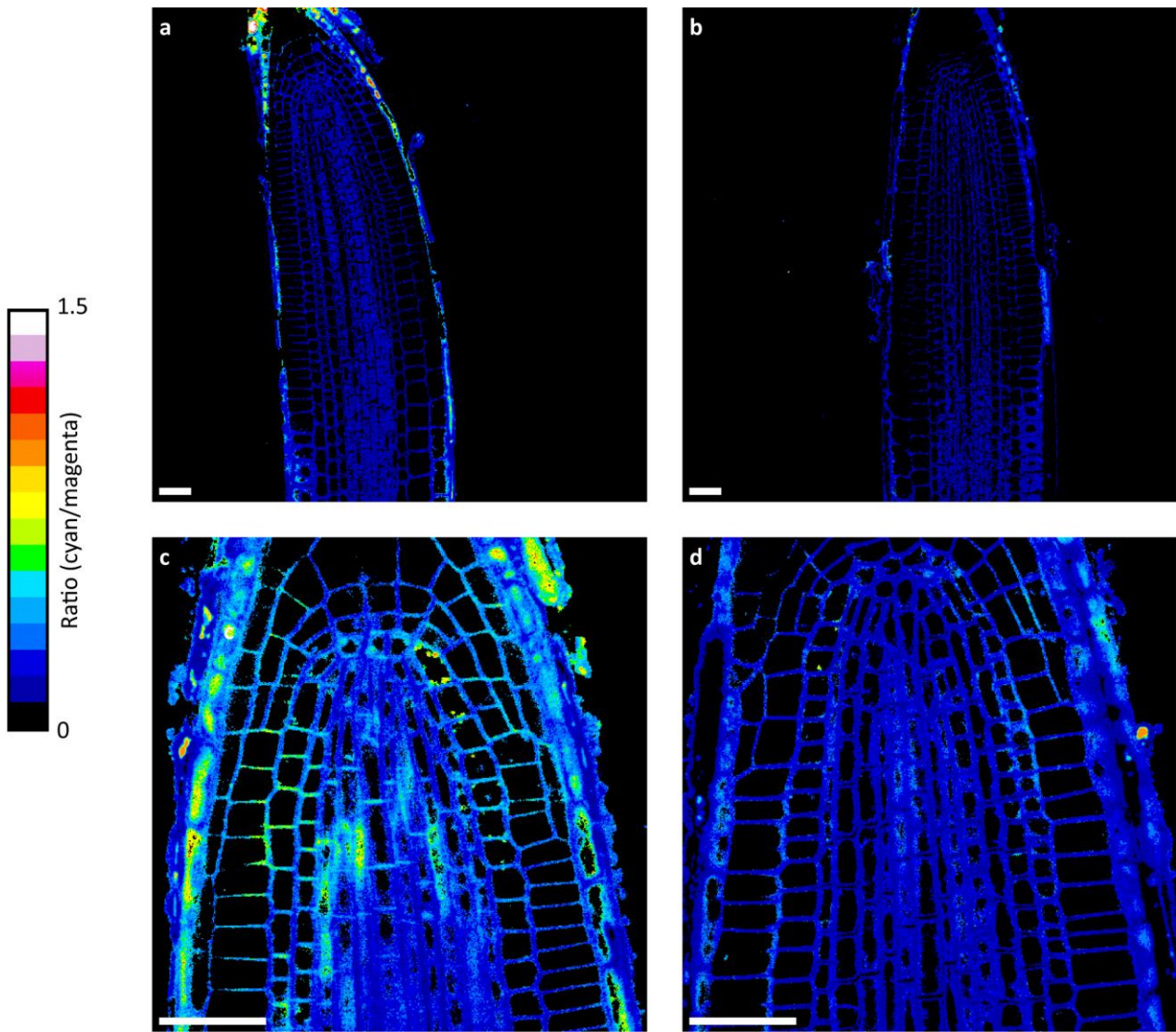


Fig. S19. Mock hemin treatment with LipoTag-Ox.

a-d, Ratiometric images of Arabidopsis root tips incubated for 1 hour with DMSO and ethanol (10 μ l DMSO and 8 μ l ethanol per 2 ml of 0.5x MS). Scale bars represent 25 μ m.

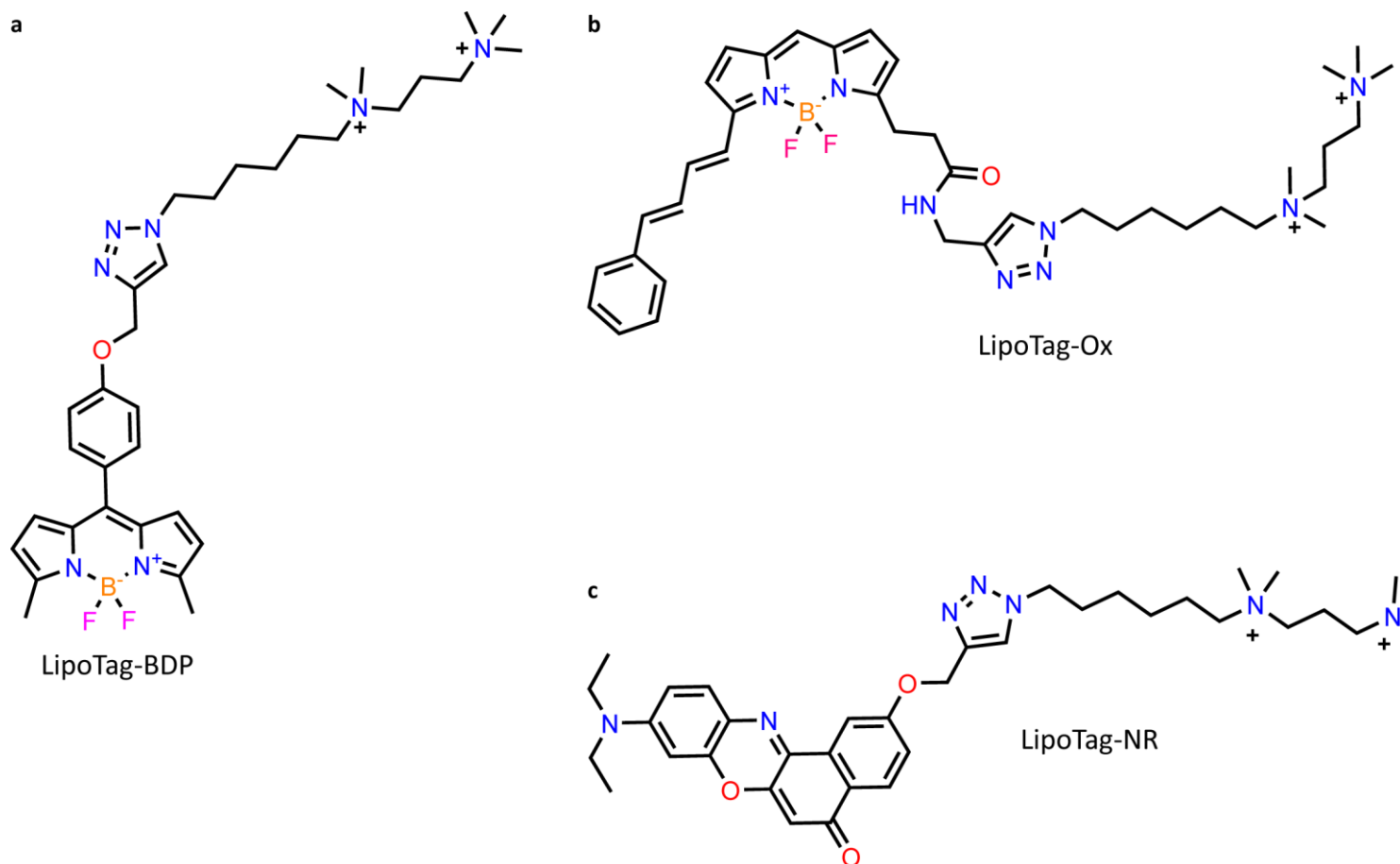


Fig. S20. Chemical structures of functional LipoTag probes.

Chemical structure of the membrane tension probe LipoTag-BDP (**a**), the membrane oxidation probe LipoTag-Ox (**b**) and the membrane order probe LipoTag-NR (**c**).

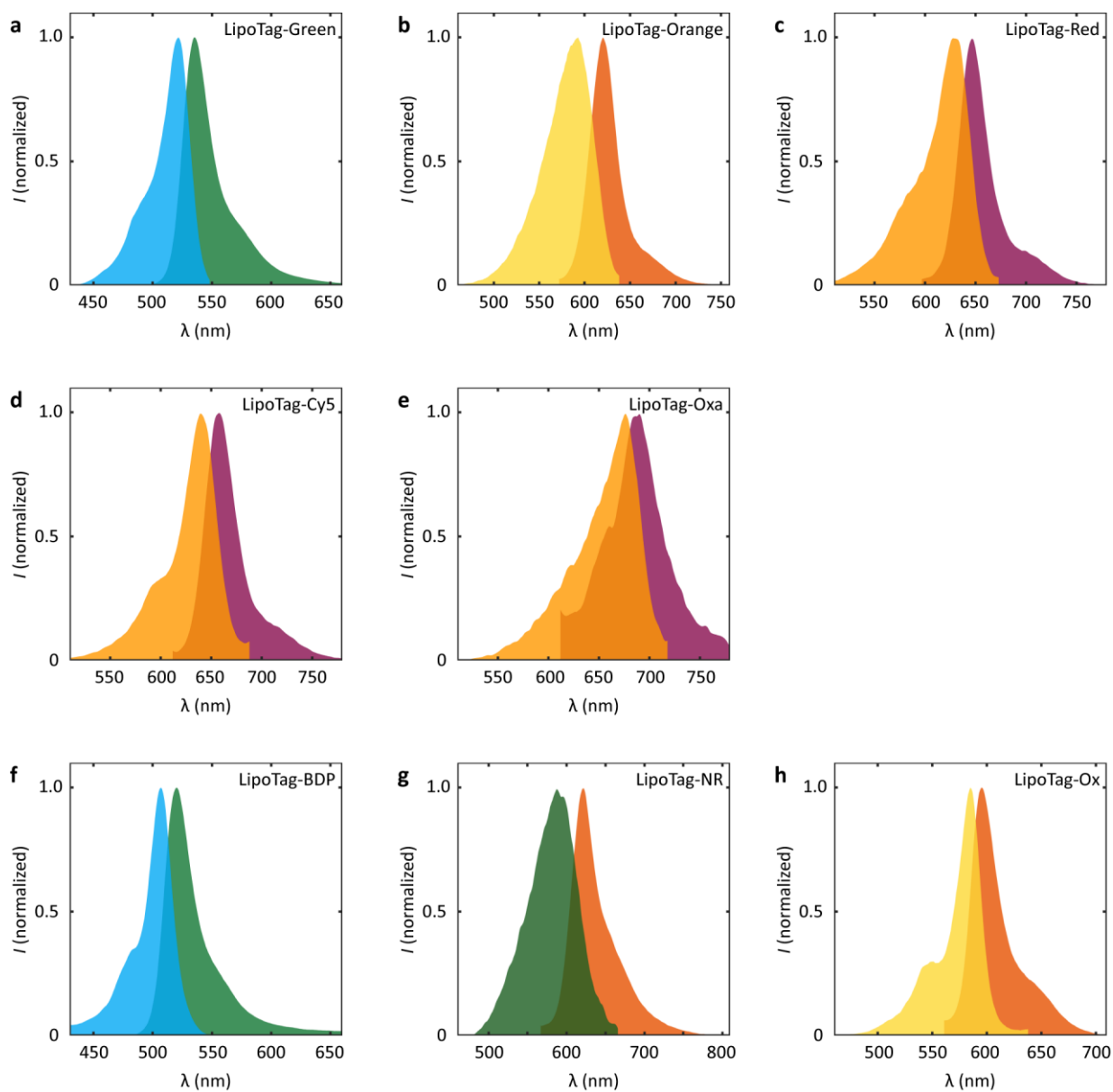


Fig. S21. Normalized fluorescence spectra of all LipoTag probes.

Normalized fluorescence excitation and emission spectra for LipoTag-Green (a), LipoTag-Orange (b), LipoTag-Red (c), LipoTag-Cy5 (d), LipoTag-Oxa (e), LipoTag-BDP (f), LipoTag-NR (g) and LipoTag-Ox (h).

Number of samples and observations

Table S1. Number of samples, multiple cells and regions were often observed per sample

Experiment	Figures	Sample numbers
Arabidopsis root imaging (non-functional)	Fig. 1b-d Fig. 2a,b Fig. S1a-t Fig. S10a-f Fig. S18a,b	LipoTag-Green n>20 LipoTag-Orange n>20 LipoTag-Red n>20 LipoTag-Cy5 n=2 LipoTag-Oxa n=2 FM1-43 n=2 DiD n=2 DiA n=2 BDP-green alkyne n=2 BDP-TR n=2 BDP630/650 n=2 BDP-rotor alkyne n=2
Non-Arabidopsis imaging (non-funtional)	Fig. 2d-o Fig. S11a-f Fig. S12a-k Fig. S13a-g Fig. S14a-f Fig. S15a-f	<i>C. richardii</i> n=2 <i>M. polymorpha</i> n=4 <i>S.rigidula</i> n=4 <i>Ectocarpus sp</i> n=5 <i>F. serratus</i> n=3 <i>S. latissimi</i> n=3 <i>S. Pombe</i> n=4 <i>V. dahliae</i> n=6 <i>E. coli</i> n>10 <i>M. musculus</i> n>10
Multicolor imaging	Fig 2p,q	n=6
FRAP	Fig. 1e	LipoTag-Green n=14 LipoTag-Orange n=20 LipoTag-Red n=19 FM4-64 n=16
Toxicity assay	Fig. 1f	n>5 wells with >10 protoplasts per well
ABA treatment stomata LipoTag-BDP FLIM	Fig. 3c-e	Open (non-treated) n=19 Closed (treated) n=20
Ablation LipoTag-BDP FLIM	Fig. 3f-h	n=9
Sterol depletion M β CD LipoTag-NR ratiometric	Fig. 4c-e	Control n=6 Treated n=8
Ablation LipoTag-NR ratiometric	Fig. 4f-h	n=6
Hemin treatment LipoTag-Ox ratiometric	Fig. 5c-e Fig. S19a-d	Treated n=6 per timepoint Mock treatment n=4
Ablation LipoTag-Ox	Fig. 5f-h	Ablation n=9 Mock n=3
Tissue penetration	Fig. S3a-t Fig. S5a-j Fig. S6a-j Fig. S7a-j	LipoTag-Green n=3 LipoTag-Orange n=3 LipoTag-Red n=3 FM4-64 n=3
Concentration range	Fig. S2a-p Fig. S4a-r	LipoTag-Green n=3 LipoTag-Orange n=3 LipoTag-Red n=3 FM4-64 n=3

Plasmolysis	Fig. S9a-i	LipoTag-Green n=4 LipoTag-Orange n=6 LipoTag-Red n=5 FM4-64 n=4
Marchantia gemma plasmodesmata staining	Fig. S16a-c	Aniline blue n = 3 Aniline blue + LT-Red n = 3 LT-Red = 3
LipoTag-BDP calibration FLIM	Fig. S17	n=5 per point

NMR spectra

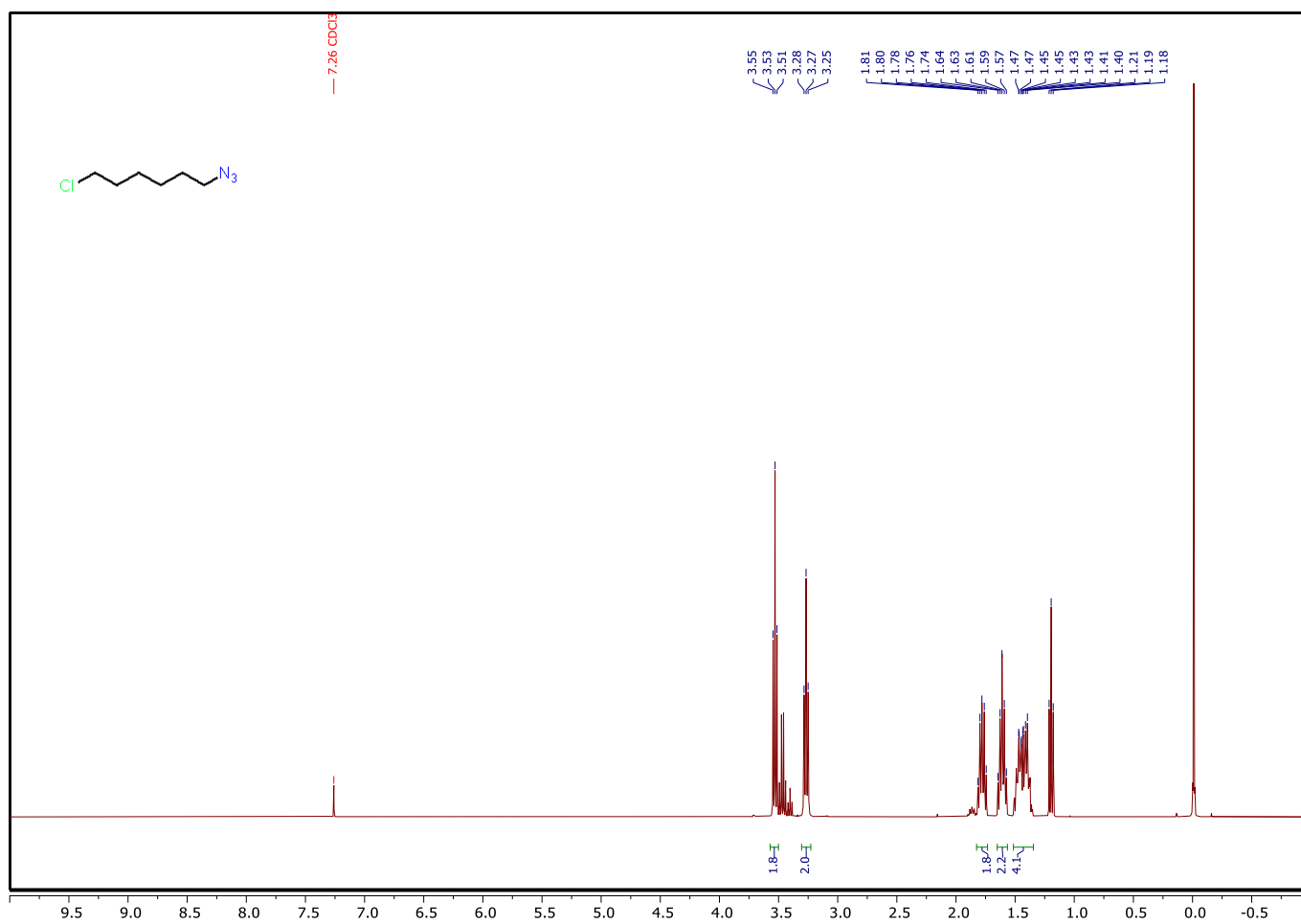


Fig. S22. ¹H spectrum of **1**.

¹H NMR (400 MHz, CDCl₃) δ 3.53 (t, *J* = 6.6 Hz, 2H), 3.27 (t, *J* = 6.9 Hz, 2H), 1.83 – 1.73 (m, 2H), 1.65 – 1.56 (m, 2H), 1.51 – 1.35 (m, 4H).

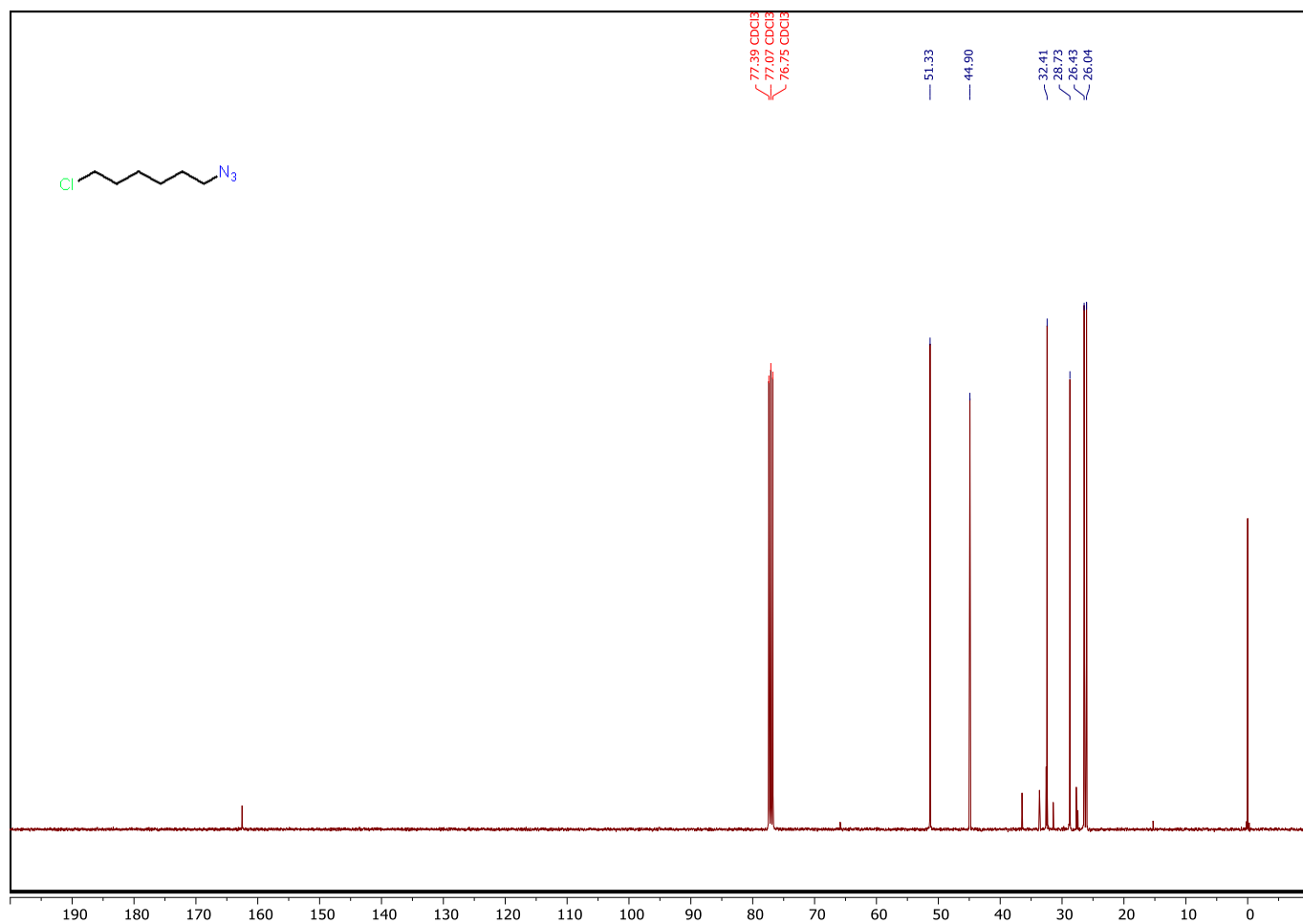


Fig. S23. ^{13}C spectrum of **1**.

^{13}C NMR (101 MHz, CDCl_3) δ 51.33, 44.90, 32.41, 28.73, 26.43, 26.04.

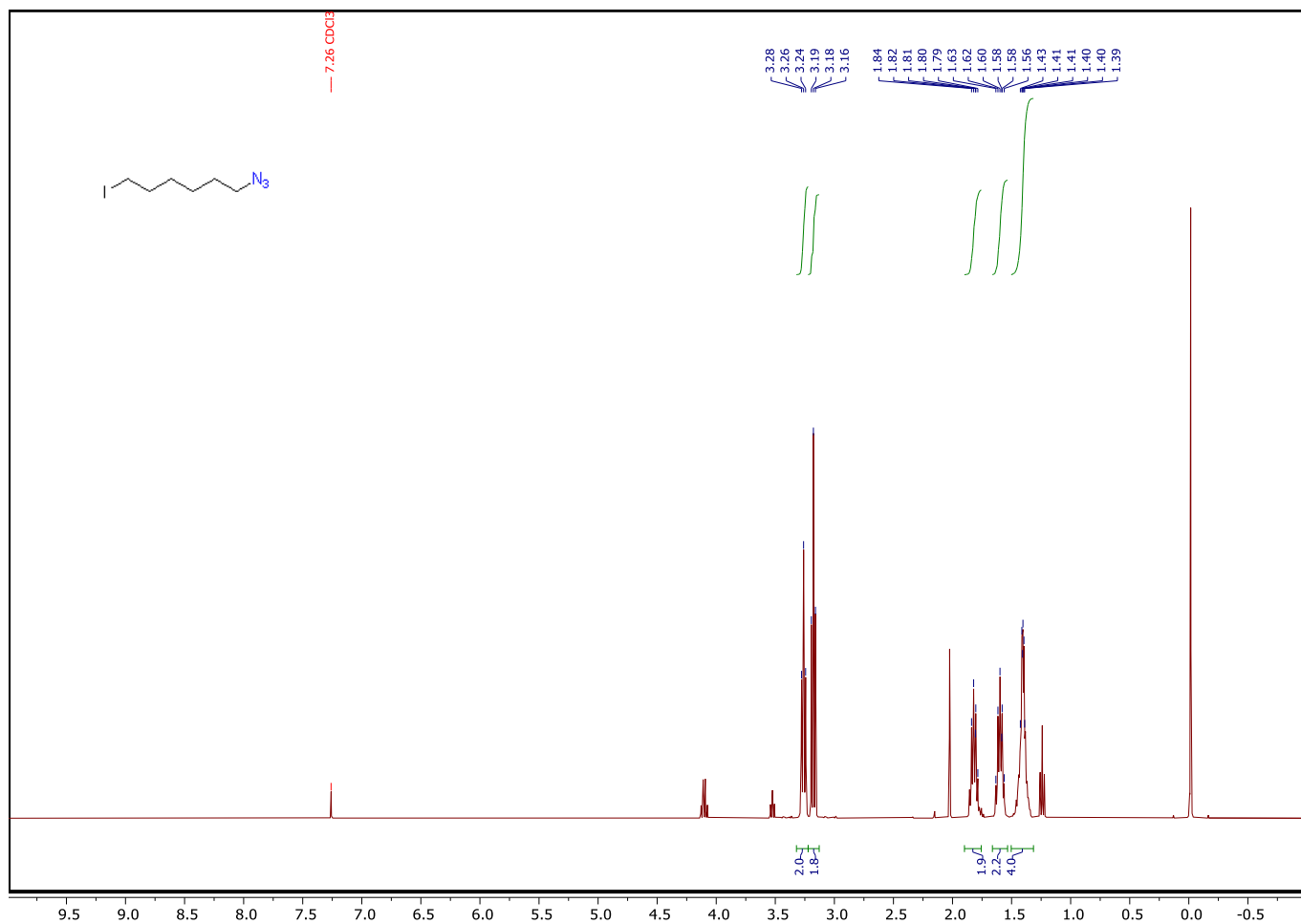


Fig. S24. ^1H spectrum of **2**.

^1H NMR (400 MHz, CDCl_3) δ 3.26 (t, $J = 6.9$ Hz, 2H), 3.18 (t, $J = 6.9$ Hz, 2H), 1.88 – 1.72 (m, 2H), 1.66 – 1.53 (m, 2H), 1.51 – 1.32 (m, 4H).

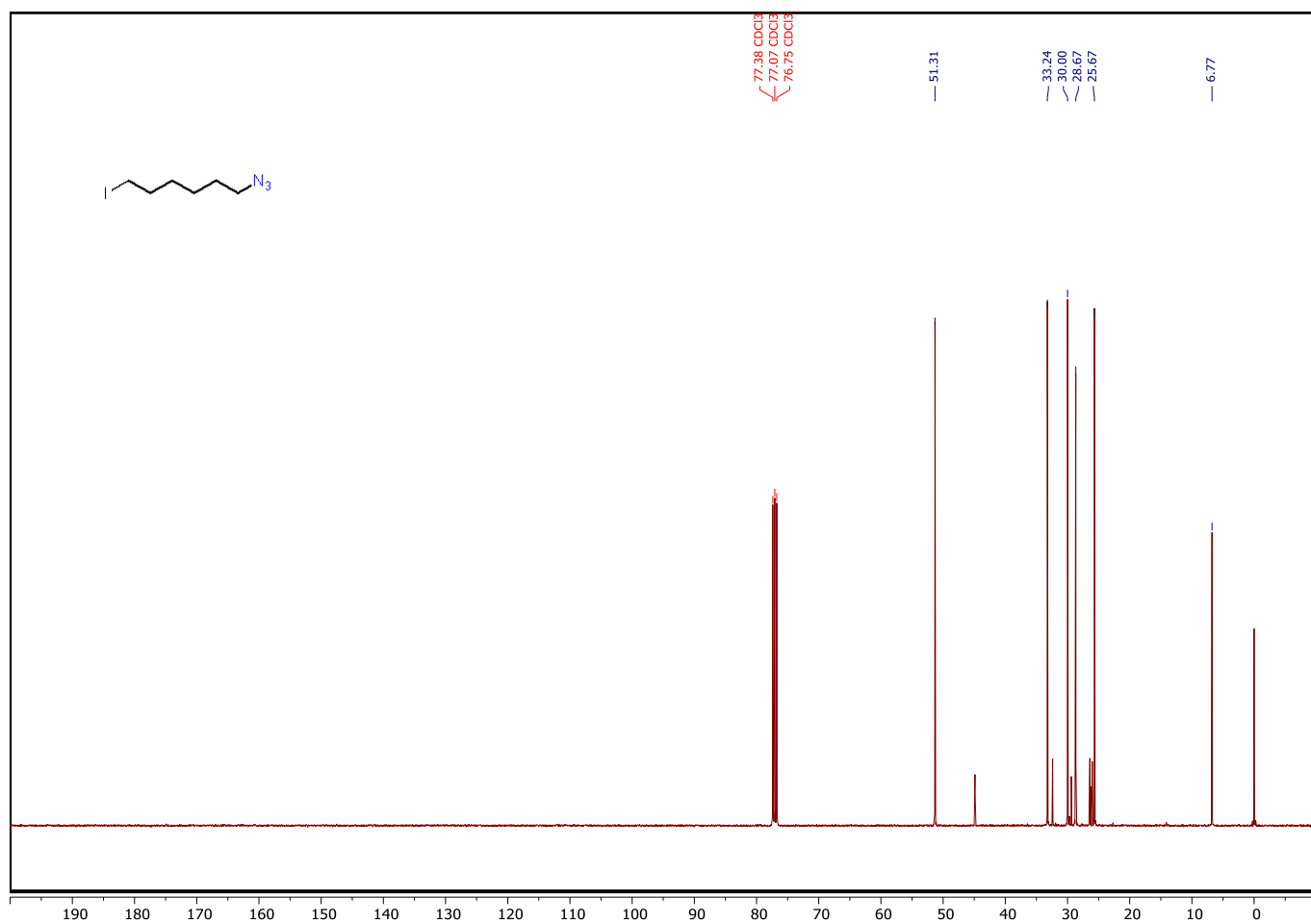


Fig. S25. ^{13}C spectrum of **2**.

^{13}C NMR (101 MHz, CDCl_3) δ 51.31, 33.24, 30.00, 28.67, 25.67, 6.77.

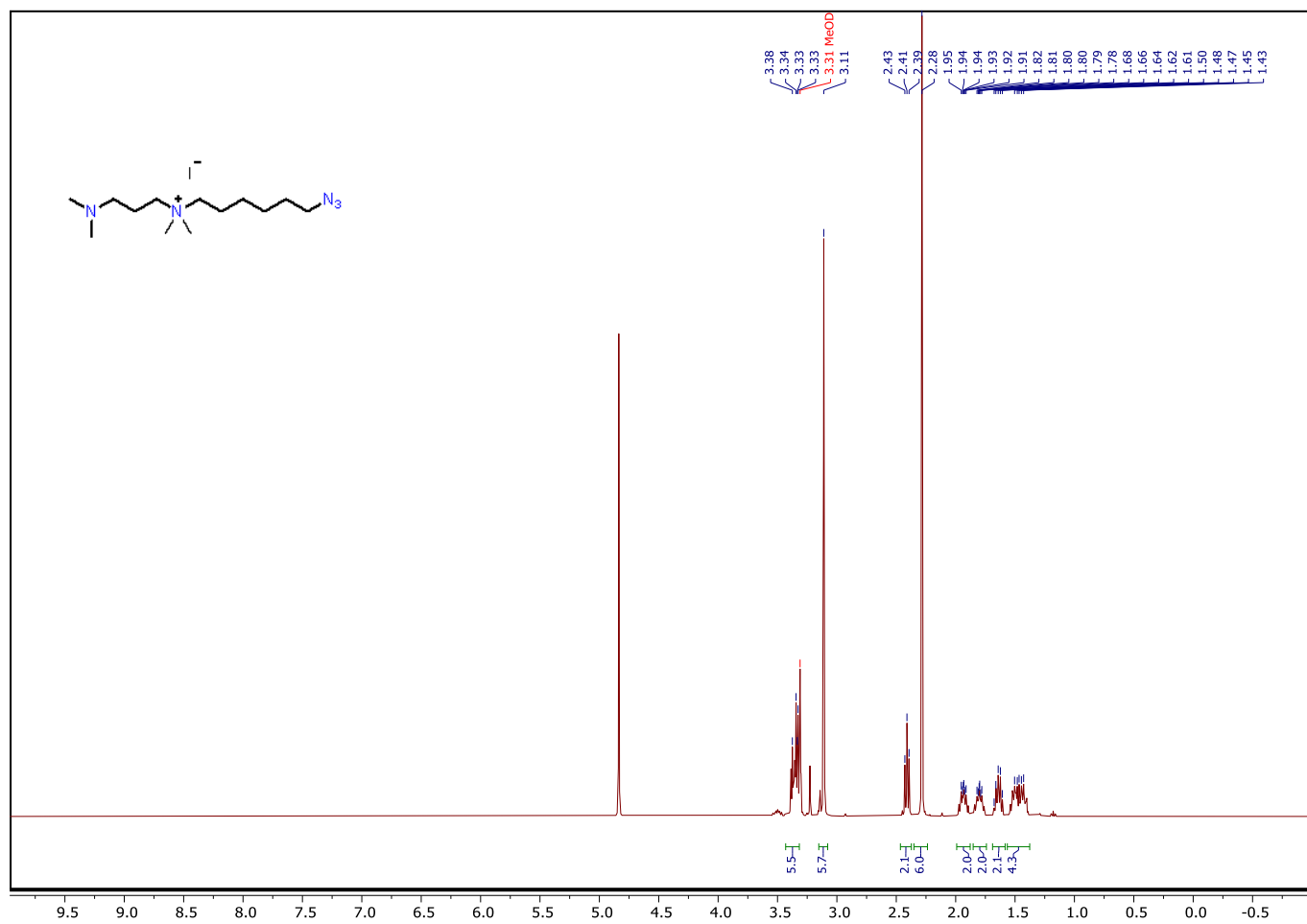


Fig. S26. ¹H spectrum of **3**.

¹H NMR (400 MHz, MeOD) δ 3.43 – 3.32 (m, 6H), 3.11 (s, 6H), 2.41 (t, $J = 7.1$ Hz, 2H), 2.28 (s, 6H), 1.99 – 1.88 (m, 2H), 1.85 – 1.74 (m, 2H), 1.69 – 1.58 (m, 2H), 1.57 – 1.38 (m, 4H).

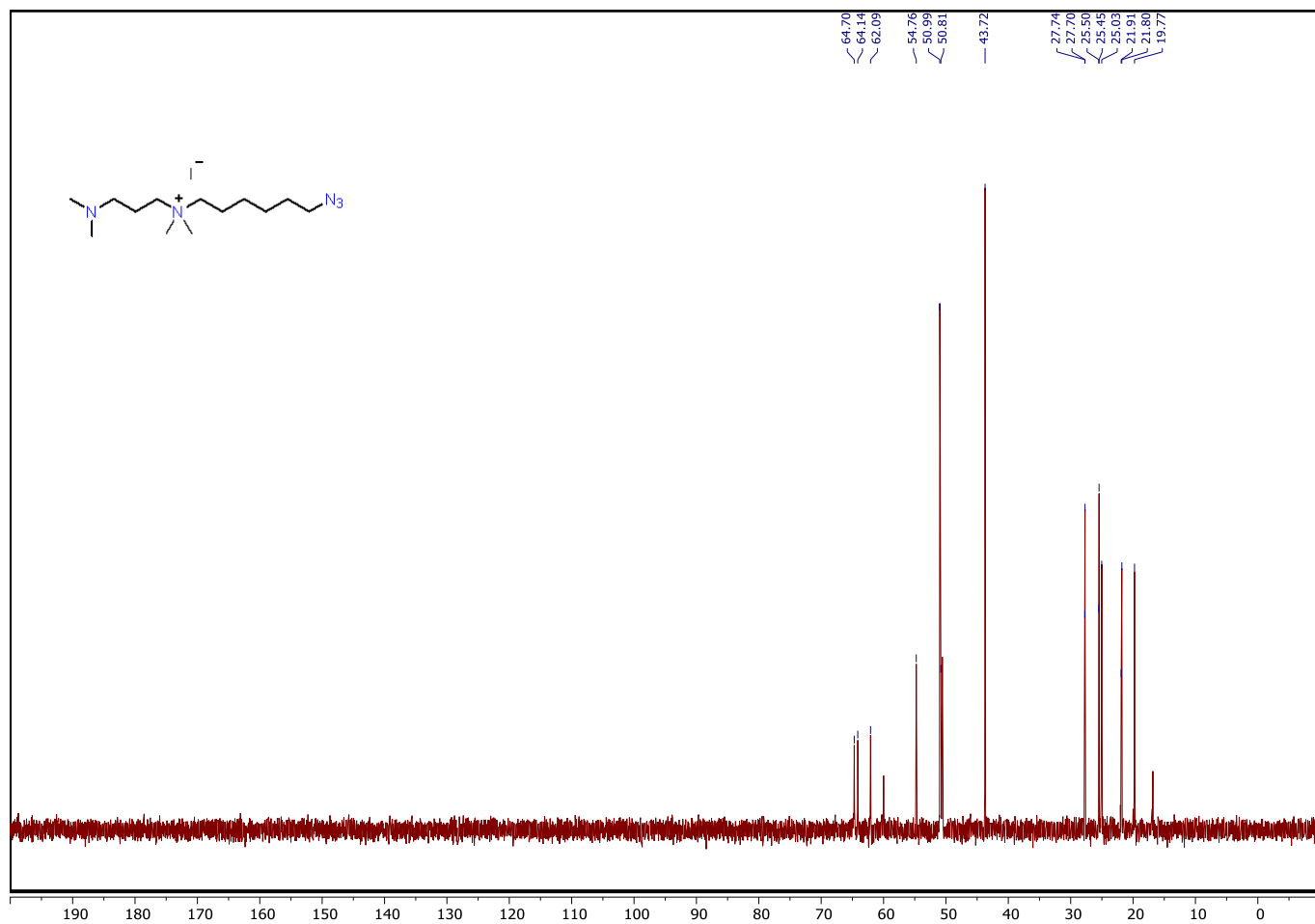


Fig. S27. ^{13}C spectrum of **3**.

^{13}C NMR (101 MHz, D_2O) δ 64.70, 64.14, 62.09, 54.76, 50.99, 50.81, 43.72, 27.74, 27.70, 25.50, 25.45, 25.03, 21.91, 21.80, 19.77.

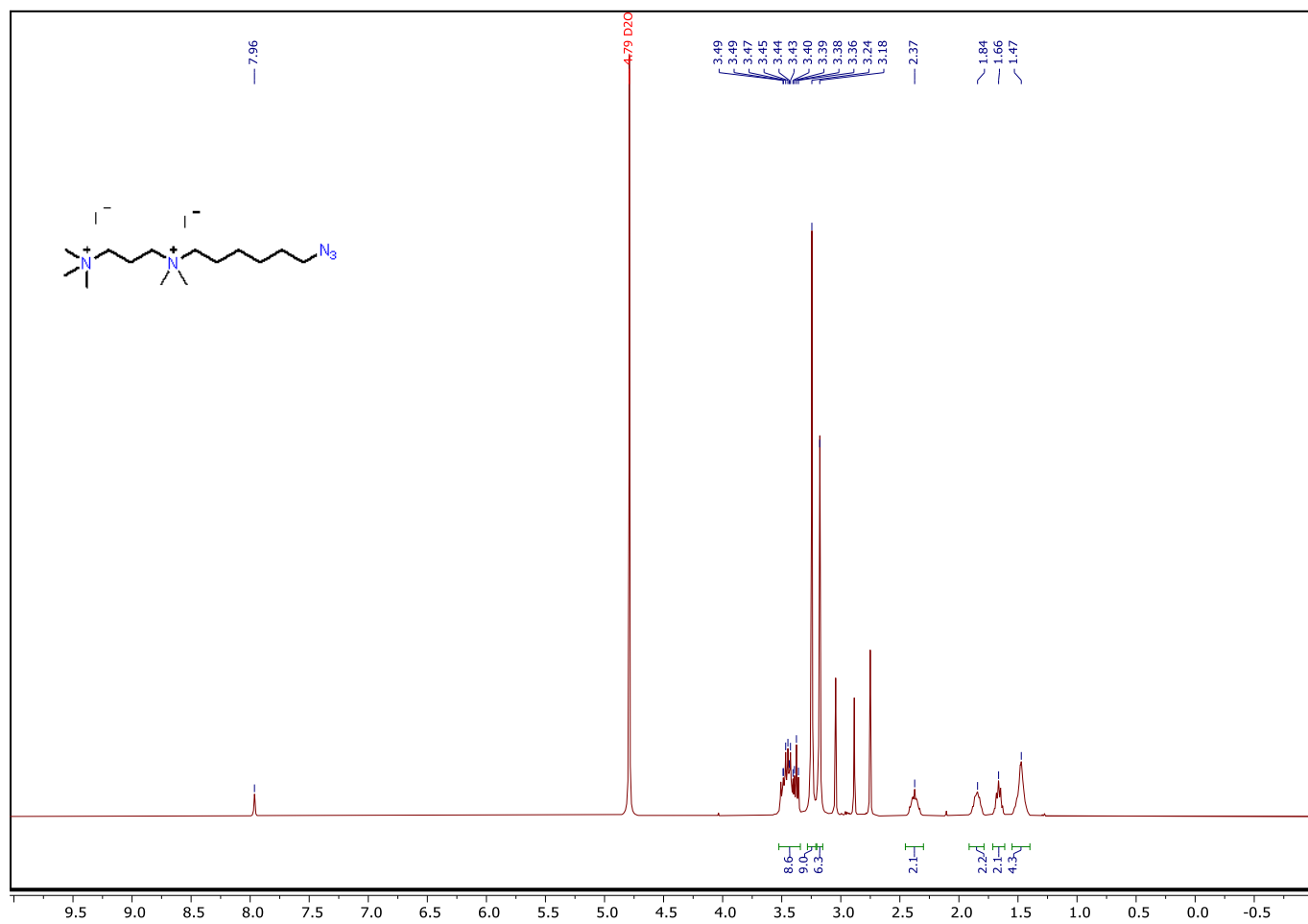


Fig. S28. ¹H spectrum of **4**.

¹H NMR (400 MHz, D₂O) δ 3.52 – 3.34 (m, 9H), 3.24 (s, 9H), 3.18 (s, 6H), 2.37 (s, 2H), 1.84 (s, 2H), 1.66 (s, 2H), 1.47 (s, 4H).

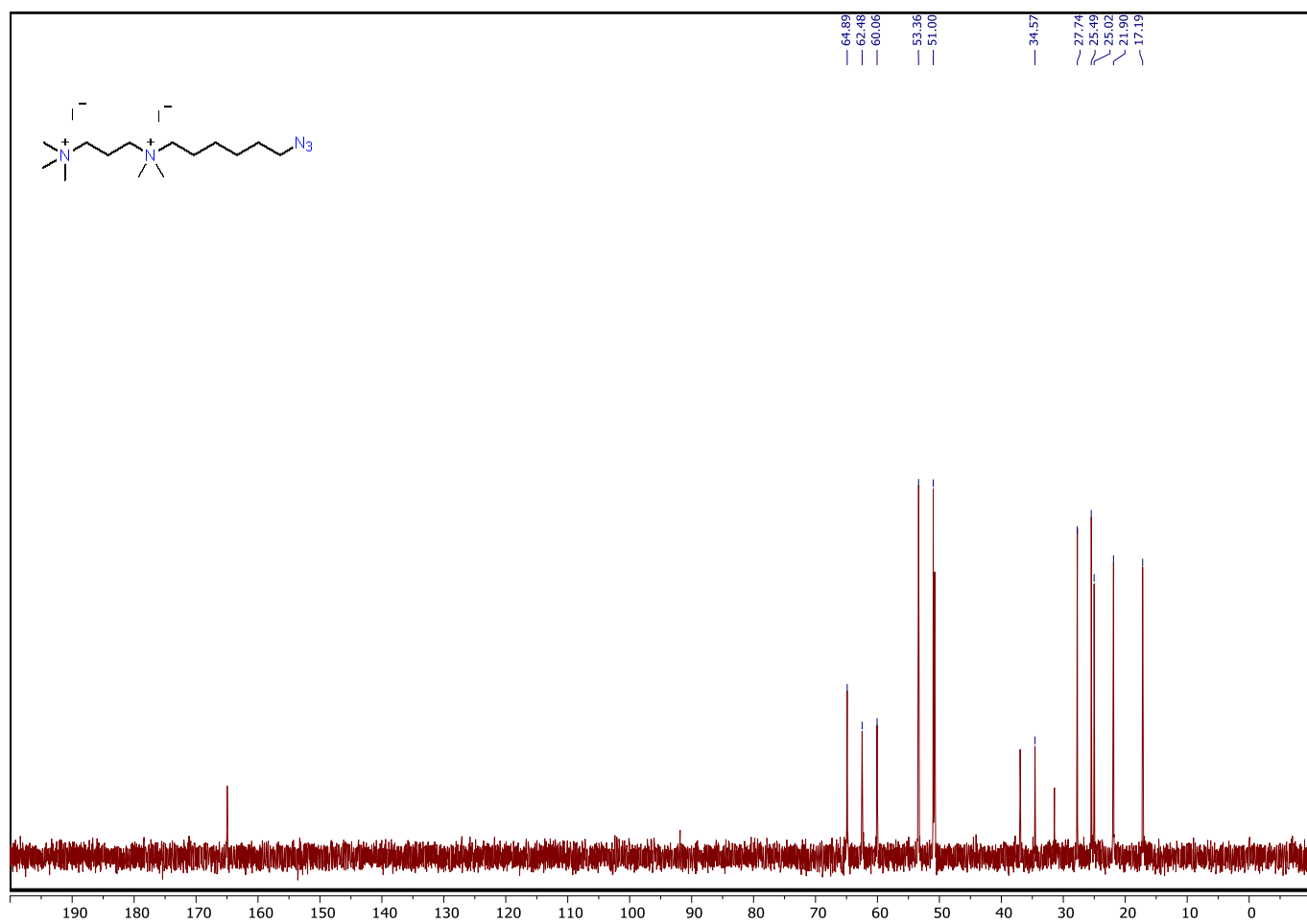


Fig. S29. ^{13}C spectrum of 4.

^{13}C NMR (101 MHz, D_2O) δ 64.89, 62.48, 60.06, 53.36, 51.00, 34.57, 27.74, 25.49, 25.02, 21.90, 17.19.

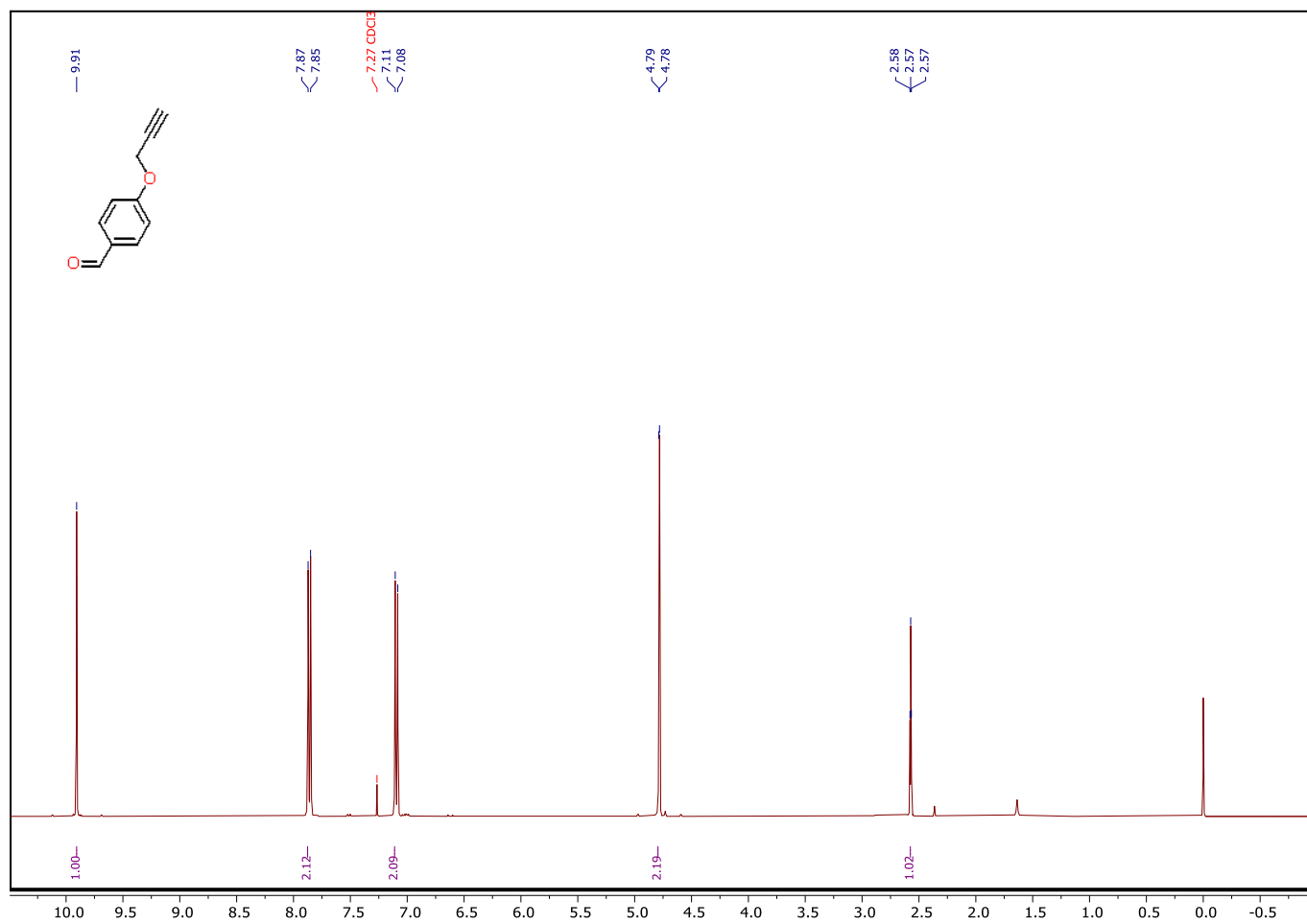


Fig. S30. ^1H spectrum of **5**.

^1H NMR (400 MHz, CDCl_3) δ 9.91 (s, 1H), 7.86 (d, $J = 8.8$ Hz, 2H), 7.09 (d, $J = 8.8$ Hz, 2H), 4.78 (d, $J = 2.4$ Hz, 2H), 2.57 (t, $J = 2.4$ Hz, 1H).

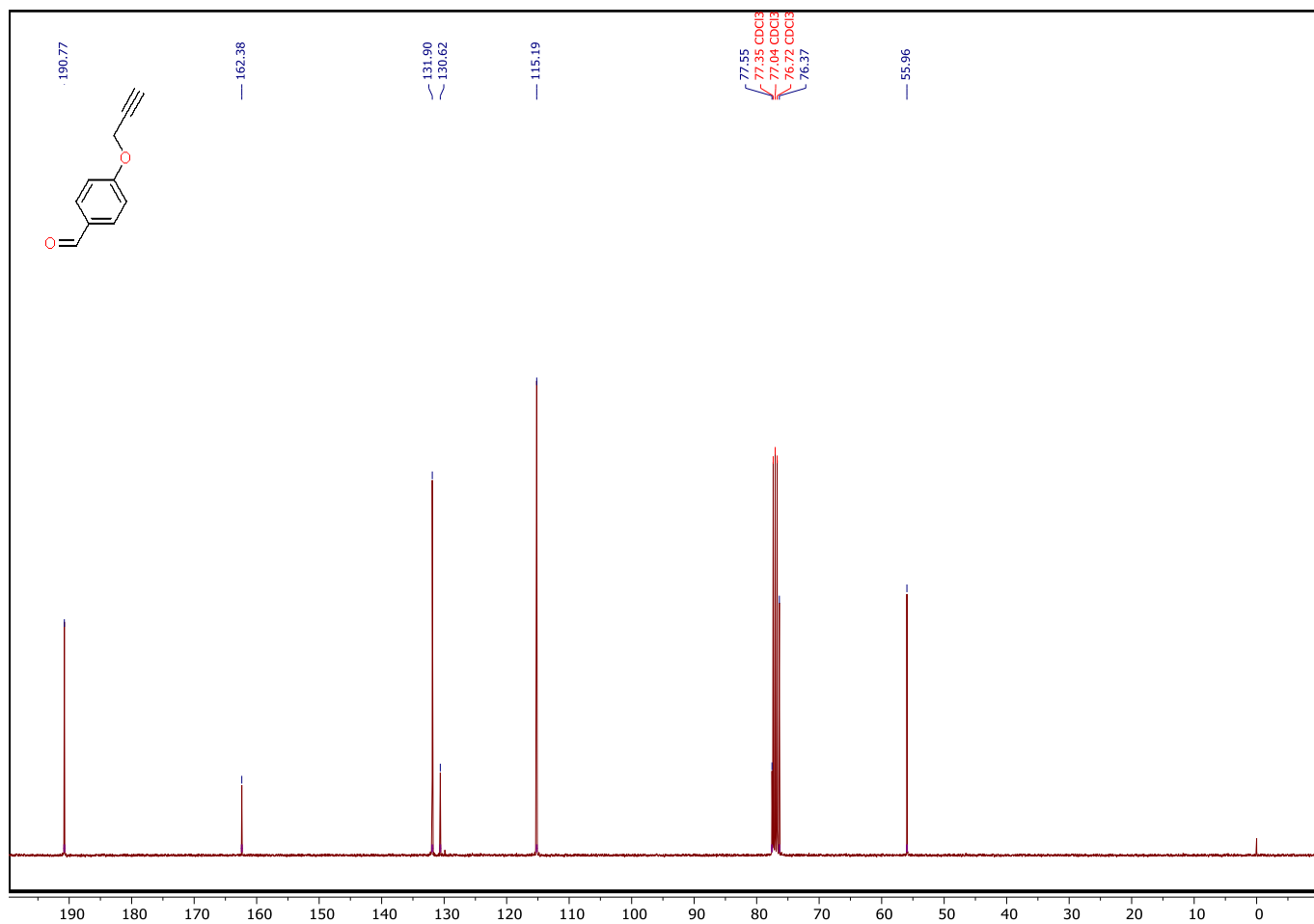


Fig. S31. ^{13}C spectrum of **5**.

^{13}C NMR (101 MHz, CDCl_3) δ 190.77, 162.38, 131.90, 130.62, 115.19, 77.55, 76.37, 55.96.

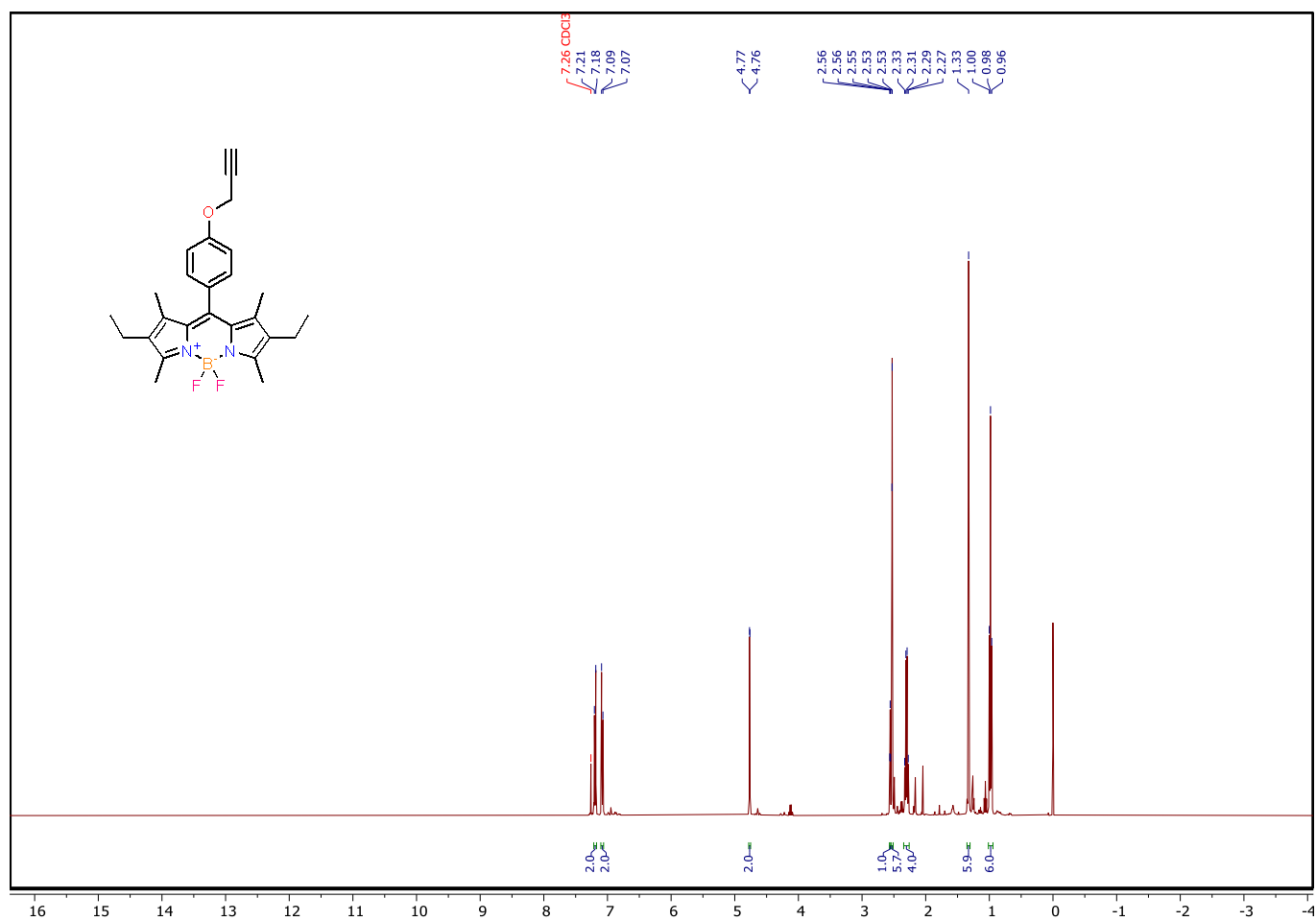


Fig. S32. ^1H spectrum of **6**.

^1H NMR (400 MHz, CDCl_3) δ 7.19 (d, J = 8.6 Hz, 2H), 7.08 (d, J = 8.7 Hz, 2H), 4.77 (d, J = 2.4 Hz, 2H), 2.56 (t, J = 2.4 Hz, 1H), 2.53 (d, J = 1.3 Hz, 6H), 2.30 (q, J = 7.5 Hz, 4H), 1.33 (s, 6H), 0.98 (t, J = 7.5 Hz, 6H).

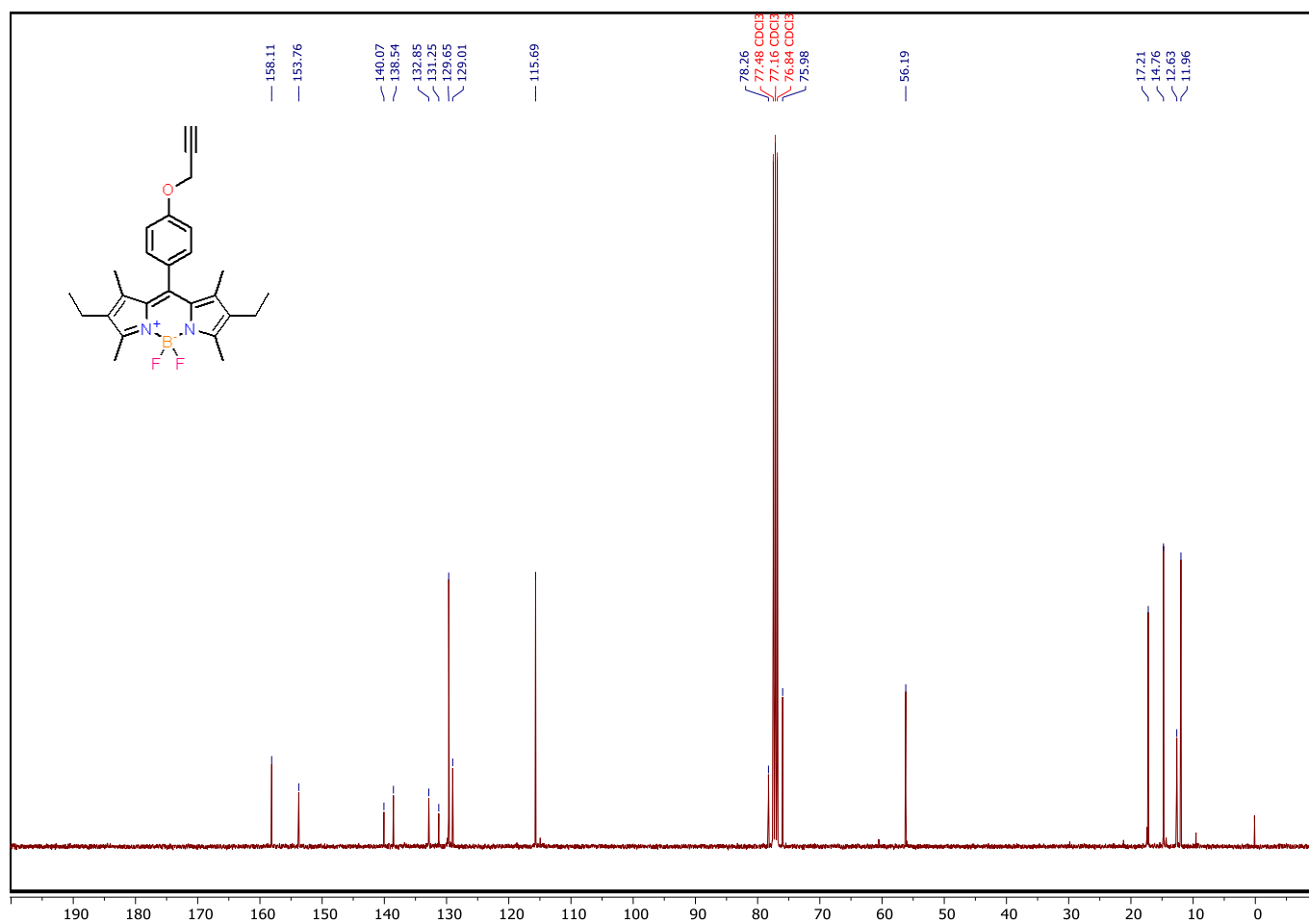


Fig. S33. ^{13}C spectrum of **6**.

^{13}C NMR (101 MHz, CDCl_3) δ 158.11, 153.76, 140.07, 138.54, 132.85, 131.25, 129.65, 129.01, 115.69, 78.26, 75.98, 56.19, 17.21, 14.76, 12.63, 11.96.

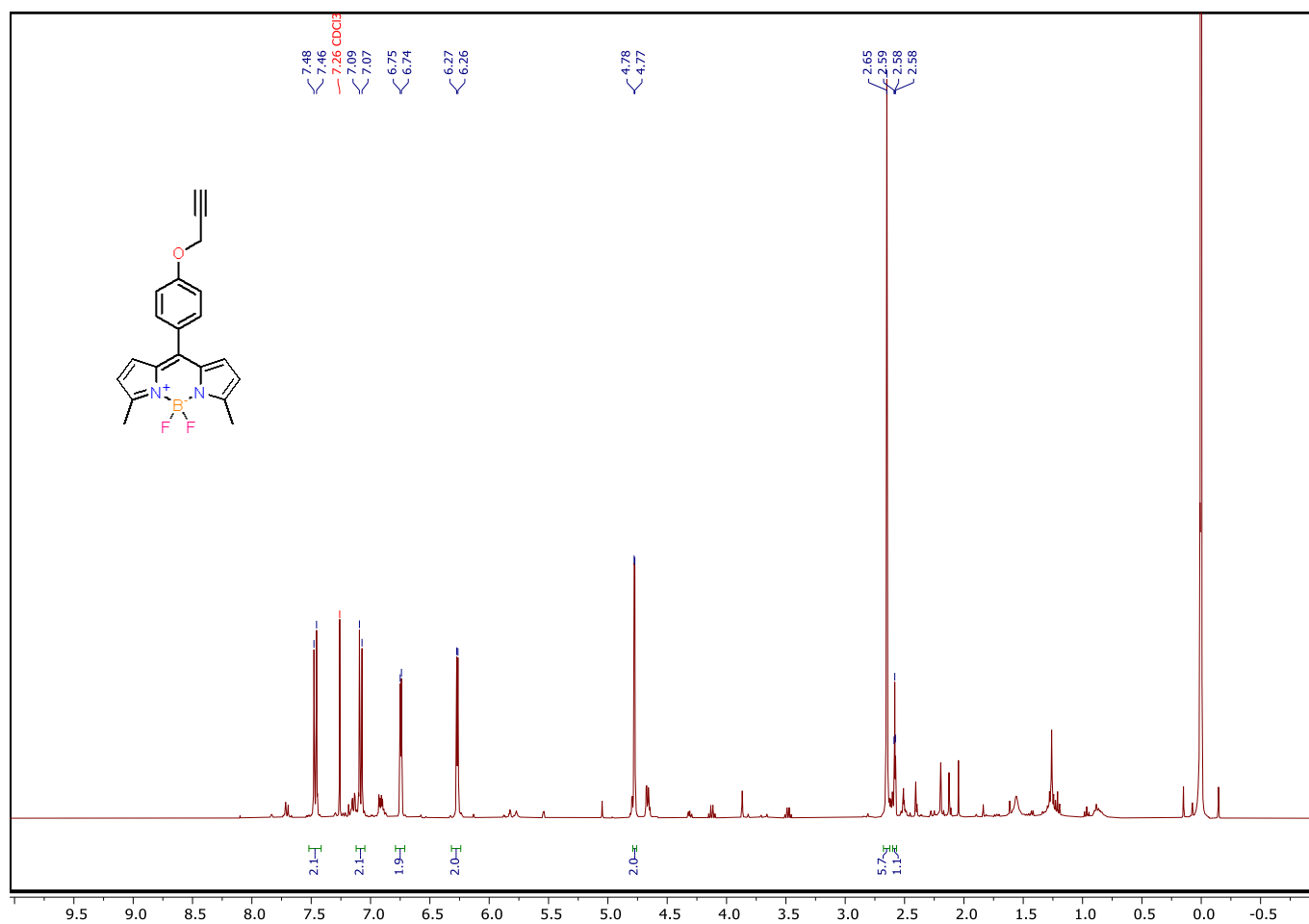


Fig. S34. ^1H spectrum of 7.

^1H NMR (400 MHz, CDCl_3) δ 7.47 (d, $J = 8.7$ Hz, 2H), 7.08 (d, $J = 8.7$ Hz, 2H), 6.74 (d, $J = 4.1$ Hz, 2H), 6.27 (d, $J = 4.2$ Hz, 2H), 4.78 (d, $J = 2.4$ Hz, 2H), 2.65 (s, 6H), 2.58 (t, $J = 2.4$ Hz, 1H).

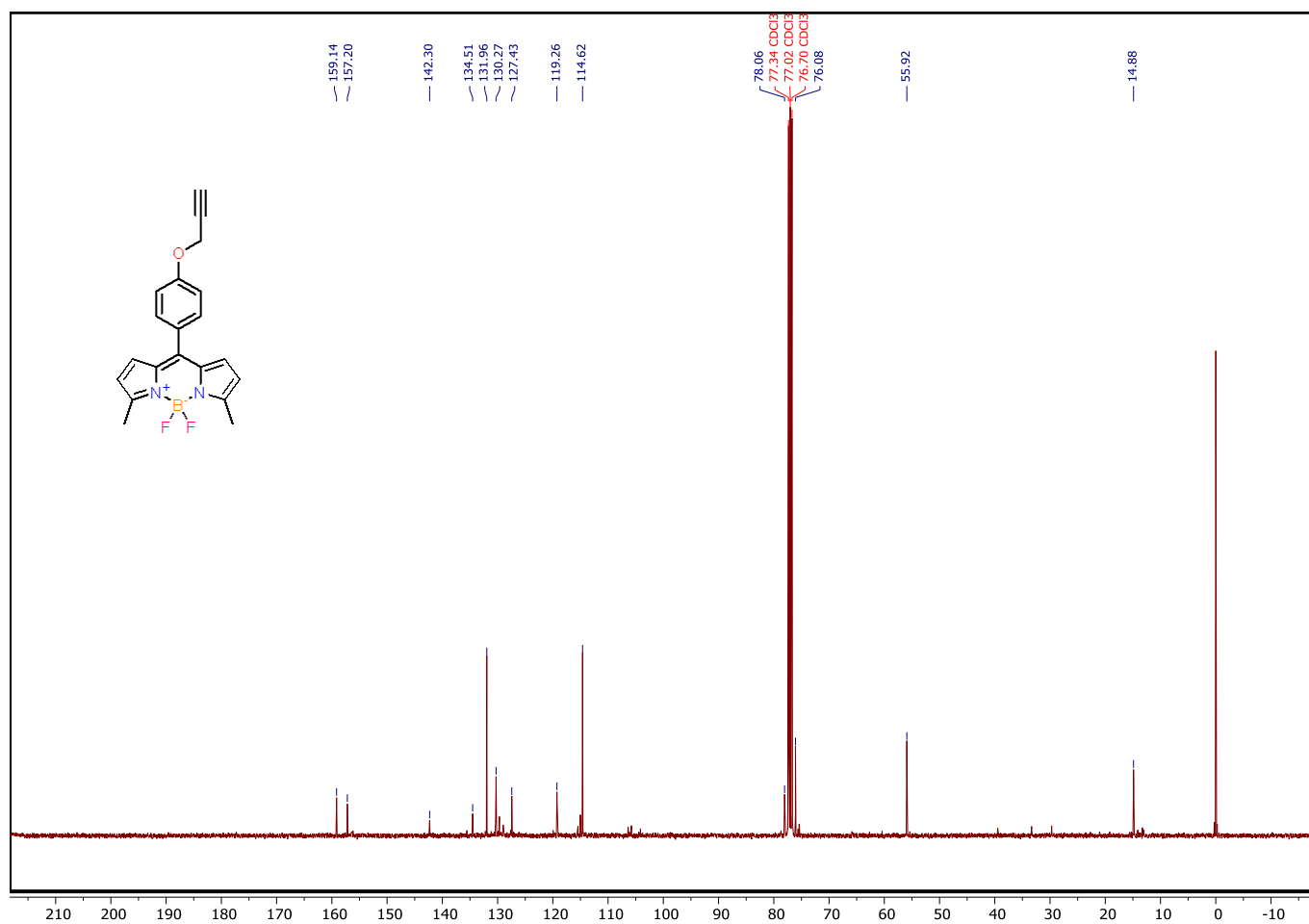


Fig. S35. ^{13}C spectrum of **7**.

^{13}C NMR (101 MHz, CDCl_3) δ 159.14, 157.20, 142.30, 134.51, 131.96, 130.27, 127.43, 119.26, 114.62, 78.06, 76.08, 55.92, 14.88.

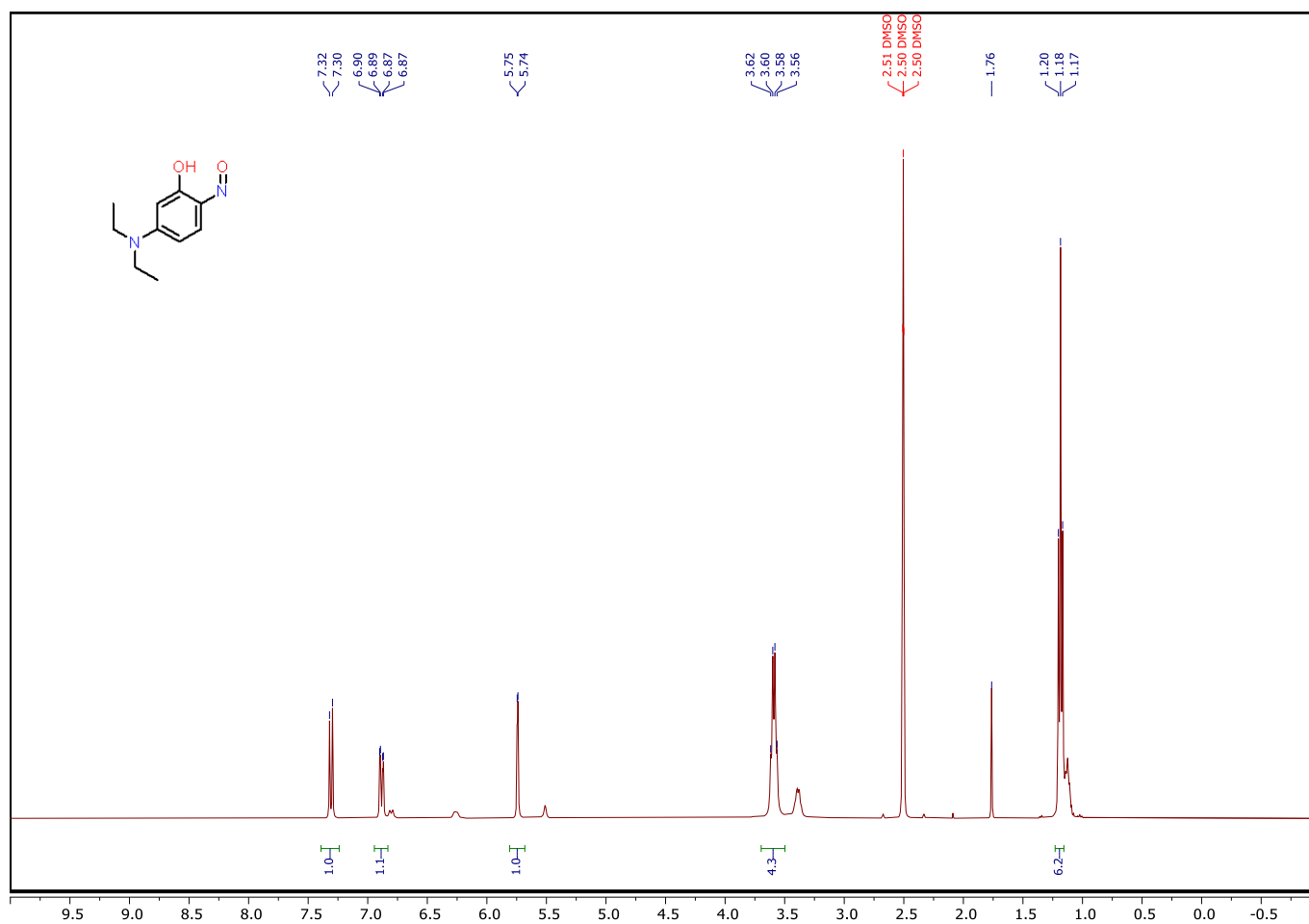


Fig. S36. ¹H spectrum of **8**.

¹H NMR (400 MHz, DMSO) δ 7.31 (d, J = 9.9 Hz, 1H), 6.88 (dd, J = 10.0, 2.6 Hz, 1H), 5.74 (d, J = 2.6 Hz, 1H), 3.59 (q, J = 7.1 Hz, 4H), 1.18 (t, J = 7.1 Hz, 6H).

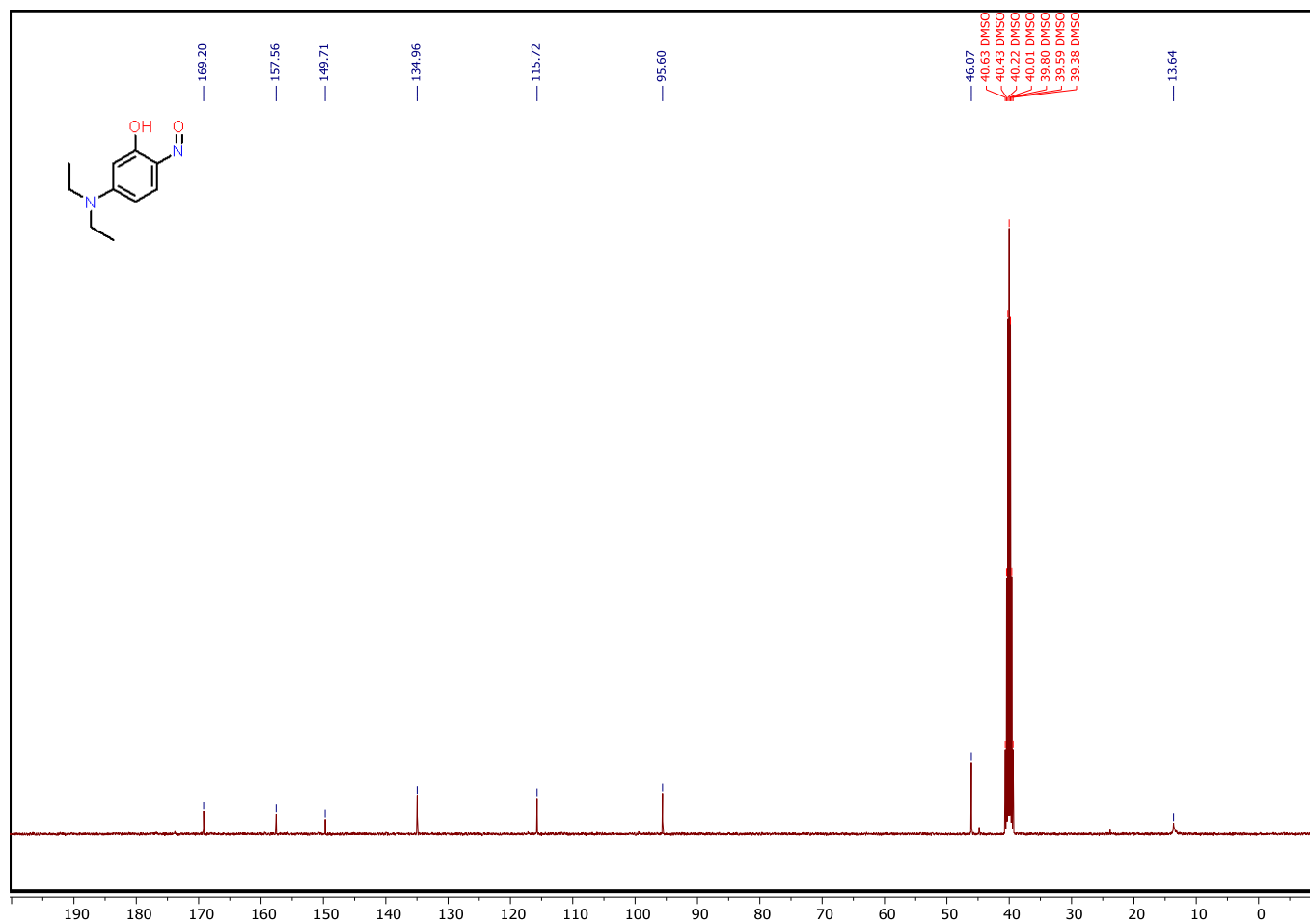


Fig. S37. ^{13}C spectrum of **8**.

^{13}C NMR (101 MHz, DMSO) δ 169.20, 157.56, 149.71, 134.96, 115.72, 95.60, 46.07, 13.64.

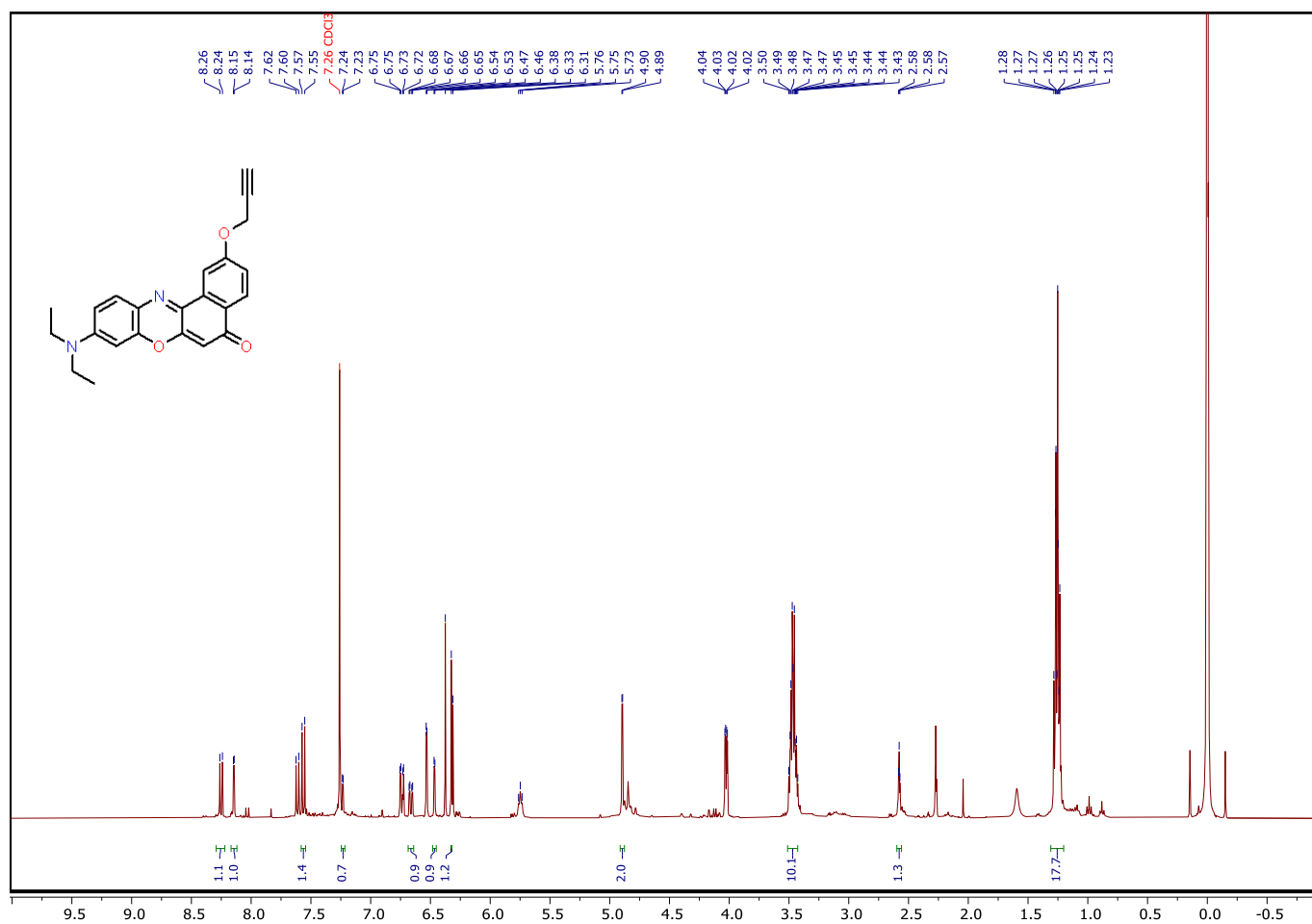


Fig. S38. ¹H spectrum of **9**.

¹H NMR (400 MHz, CDCl₃) δ 8.25 (d, *J* = 8.8 Hz, 1H), 8.14 (d, *J* = 2.6 Hz, 1H), 7.56 (d, *J* = 9.1 Hz, 1H), 7.23 (d, *J* = 2.6 Hz, 1H), 6.66 (dd, *J* = 9.0, 2.7 Hz, 1H), 6.47 (d, *J* = 2.7 Hz, 1H), 6.33 (s, 1H), 4.90 (d, *J* = 2.4 Hz, 2H), 3.47 (qd, *J* = 7.1, 4.3 Hz, 10H), 2.58 (t, *J* = 2.4 Hz, 1H), 1.26 (td, *J* = 7.1, 5.7 Hz, 18H)

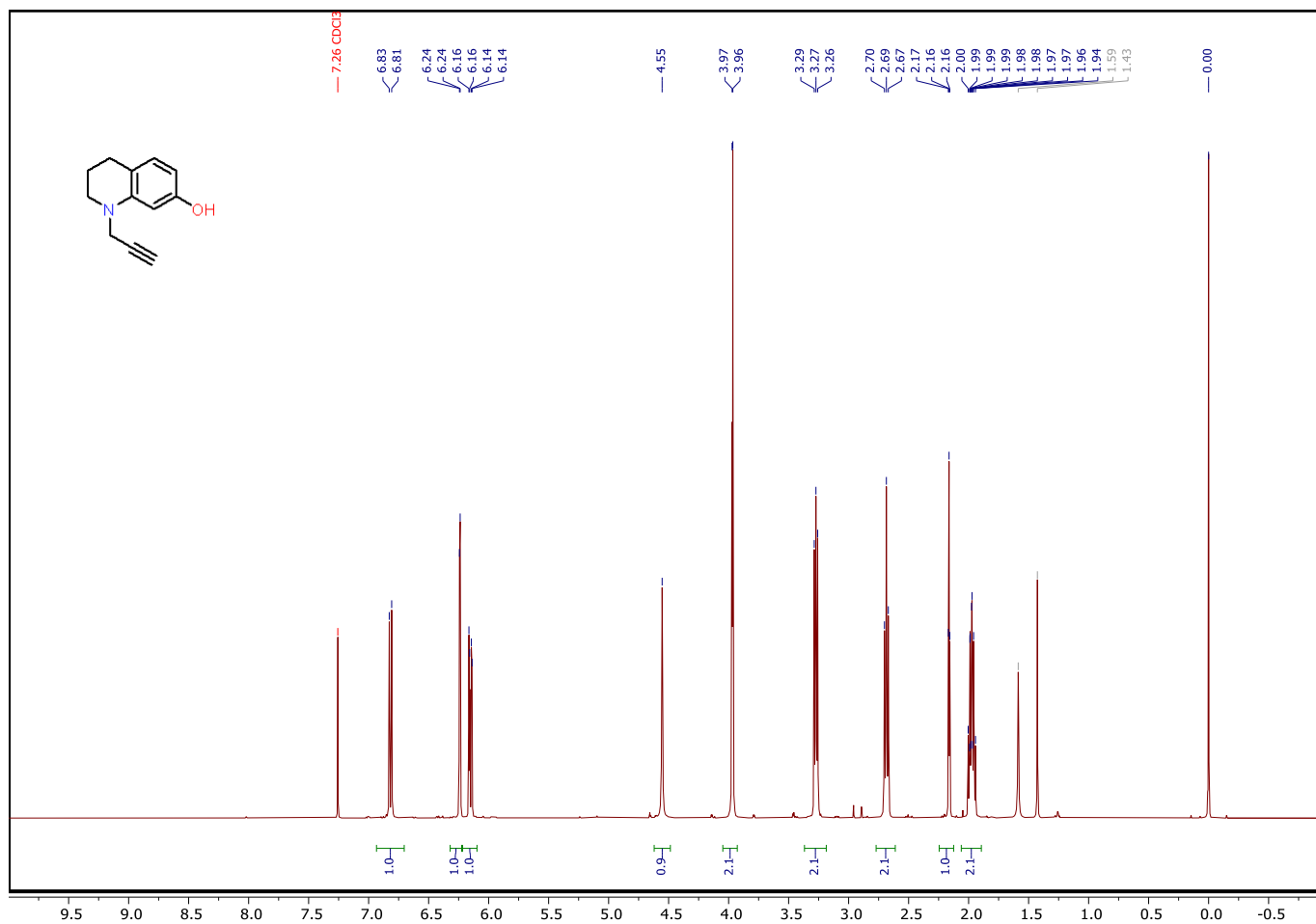


Fig. S41. ¹H spectrum of **10**.

¹H NMR (400 MHz, CDCl₃) δ 6.82 (d, J = 8.0 Hz, 1H), 6.24 (d, J = 2.4 Hz, 1H), 6.15 (dd, J = 8.0, 2.4 Hz, 1H), 4.55 (s, 1H), 3.97 (d, J = 2.4 Hz, 2H), 3.34 – 3.18 (m, 2H), 2.69 (t, J = 6.5 Hz, 2H), 2.16 (t, J = 2.4 Hz, 1H), 2.02 – 1.93 (m, 2H).

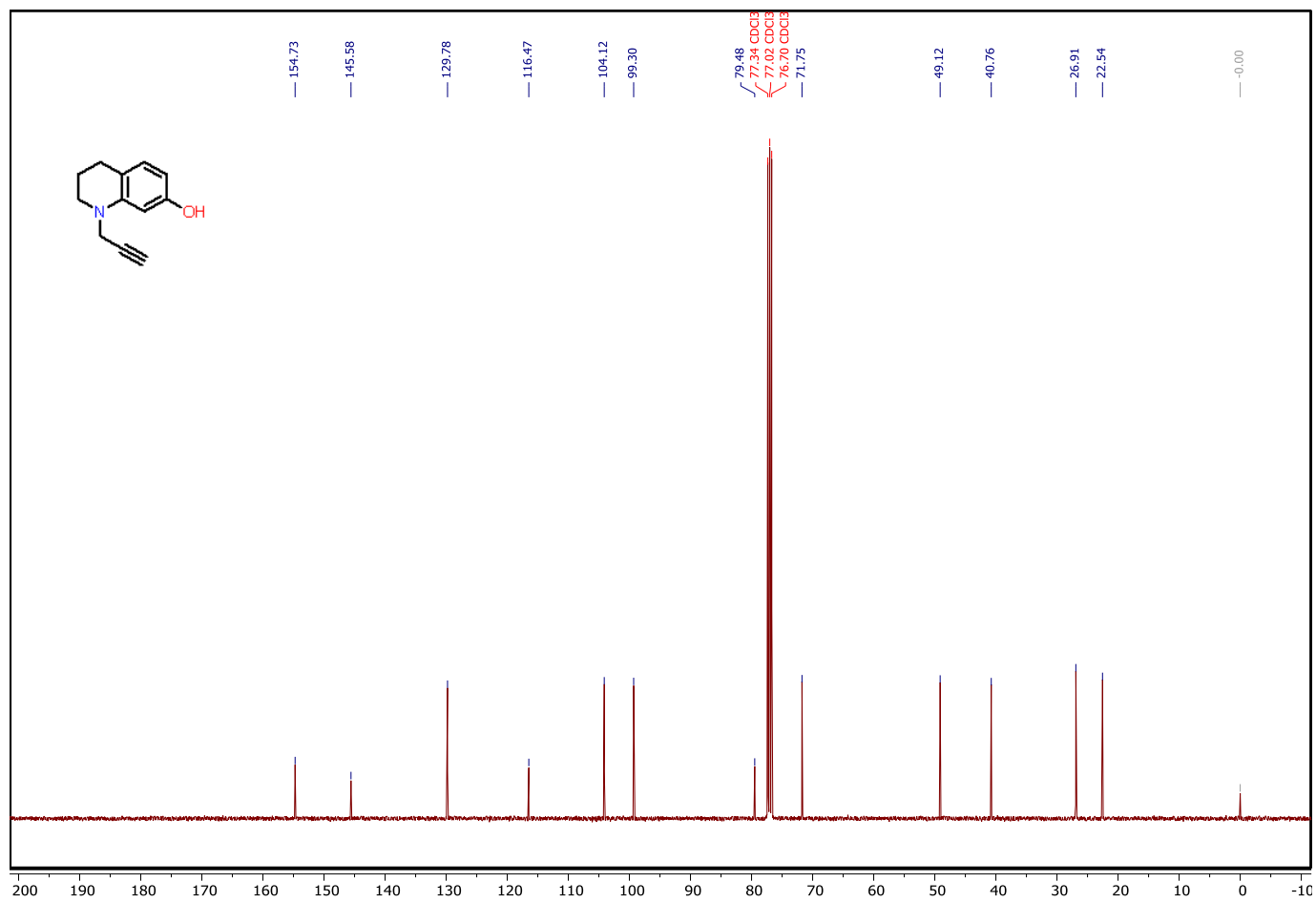


Fig. S42. ^{13}C spectrum of **10**.

^{13}C NMR (101 MHz, CDCl_3) δ 154.73, 145.58, 129.78, 116.47, 104.12, 99.30, 79.48, 71.75, 49.12, 40.76, 26.91, 22.54.

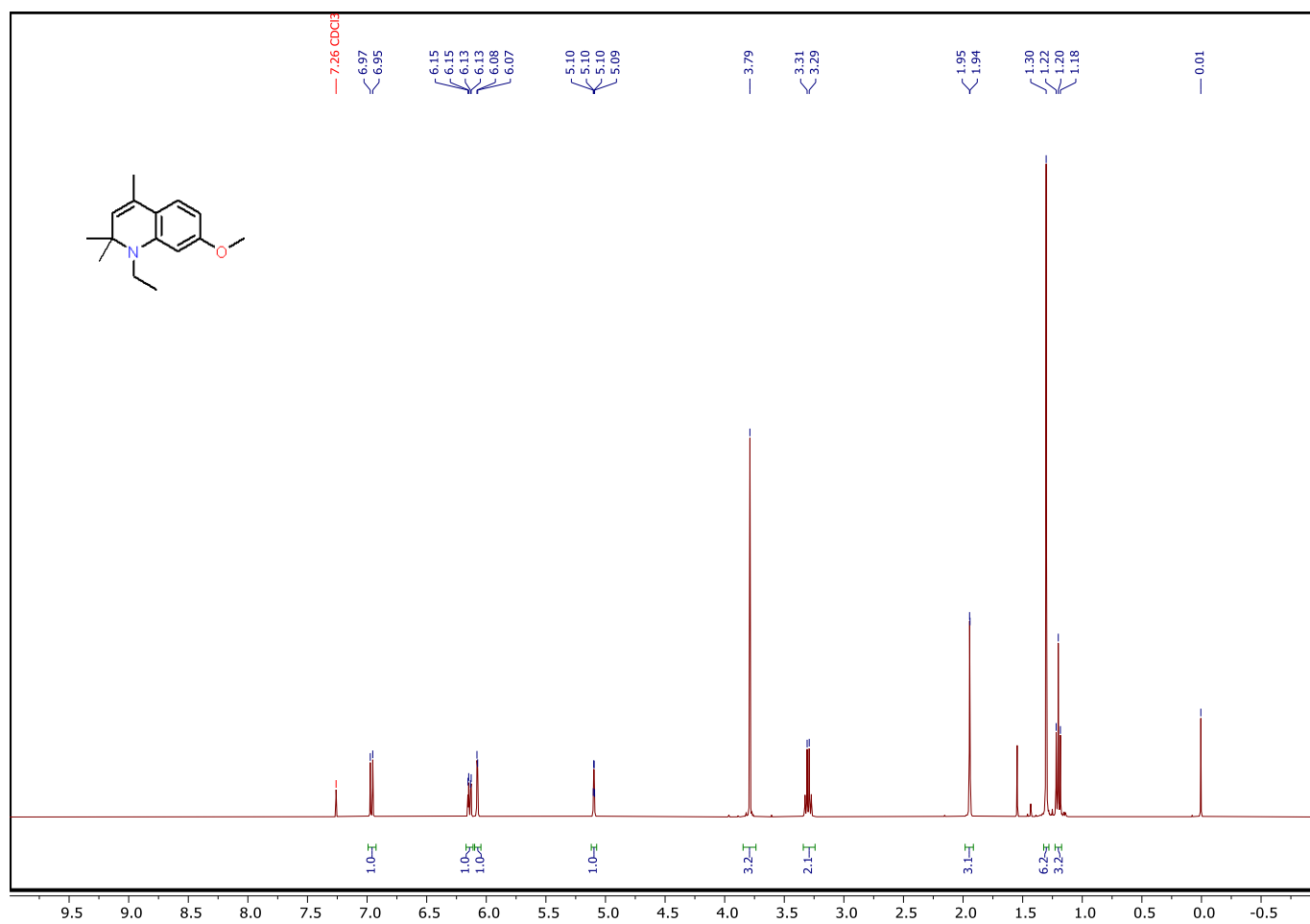


Fig. S39. ¹H spectrum of **11**.

¹H NMR (400 MHz, CDCl₃) δ 6.96 (d, *J* = 8.3 Hz, 1H), 6.14 (dd, *J* = 8.3, 2.4 Hz, 1H), 6.08 (d, *J* = 2.4 Hz, 1H), 5.10 (q, *J* = 1.4 Hz, 1H), 3.79 (s, 3H), 3.30 (d, *J* = 7.1 Hz, 2H), 1.94 (d, *J* = 1.4 Hz, 3H), 1.30 (s, 6H), 1.20 (t, *J* = 7.0 Hz, 3H).

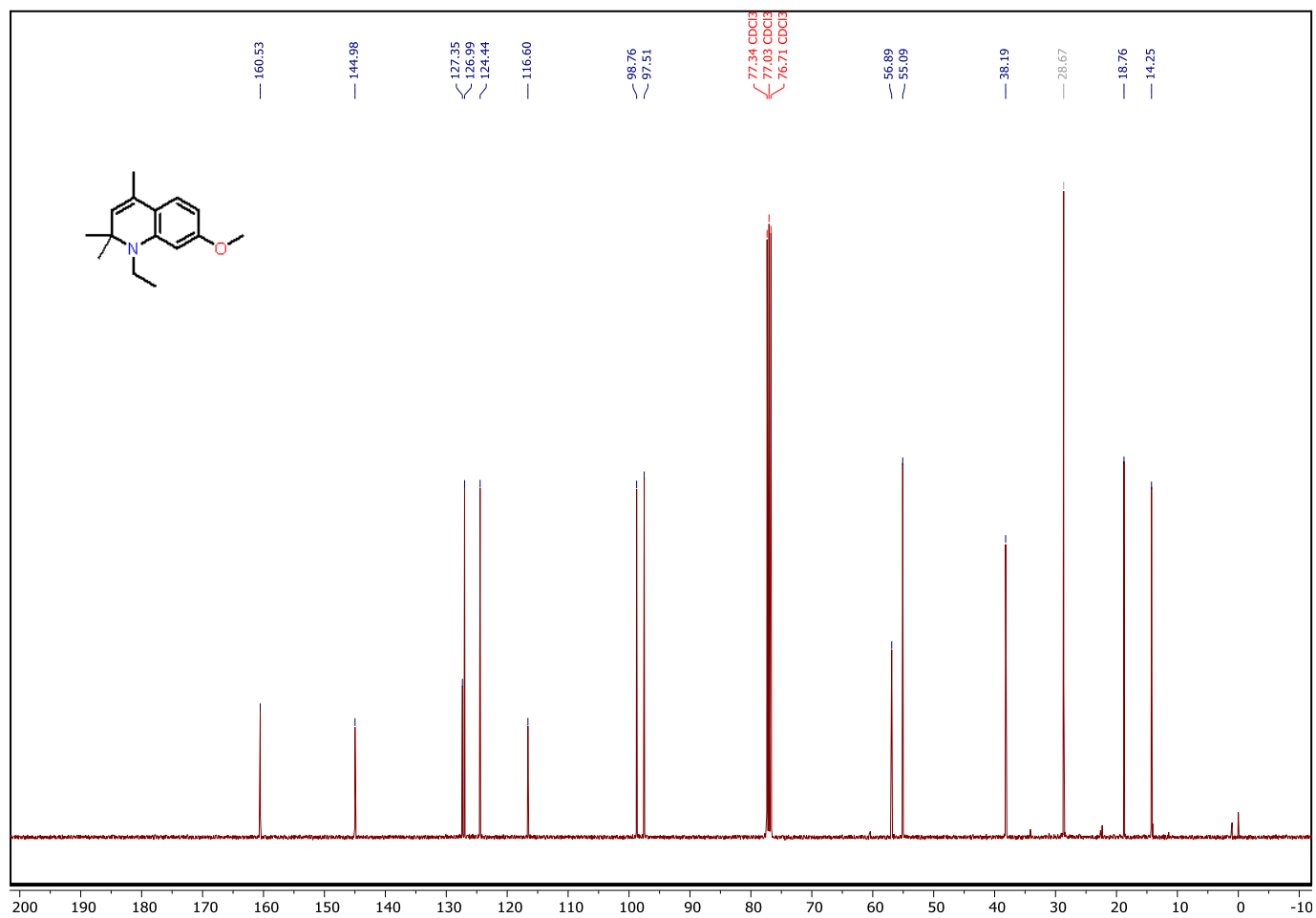


Fig. S40. ^{13}C spectrum of **11**.

^{13}C NMR (101 MHz, CDCl_3) δ 160.53, 144.98, 127.35, 126.99, 124.44, 116.60, 98.76, 97.51, 56.89, 55.09, 38.19, 18.76, 14.25.

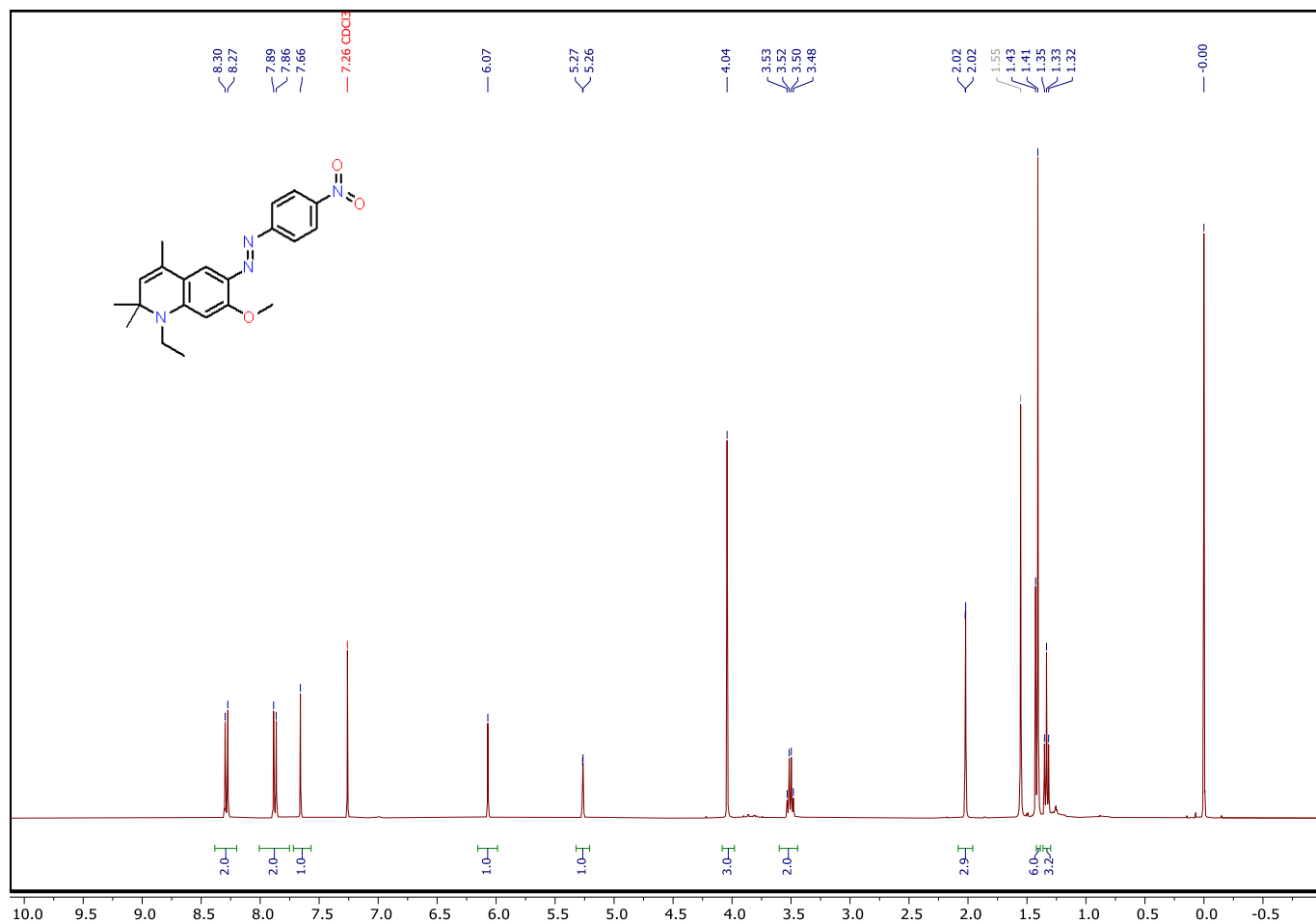


Fig. S43. ¹H spectrum of **12**.

¹H NMR (400 MHz, CDCl₃) δ 8.29 (d, J = 9.0 Hz, 2H), 7.87 (d, J = 9.0 Hz, 2H), 7.66 (s, 1H), 6.07 (s, 1H), 5.27 (d, J = 1.5 Hz, 1H), 4.04 (s, 3H), 3.51 (q, J = 7.1 Hz, 2H), 2.02 (d, J = 1.4 Hz, 3H), 1.41 (s, 6H), 1.33 (t, J = 7.0 Hz, 3H).

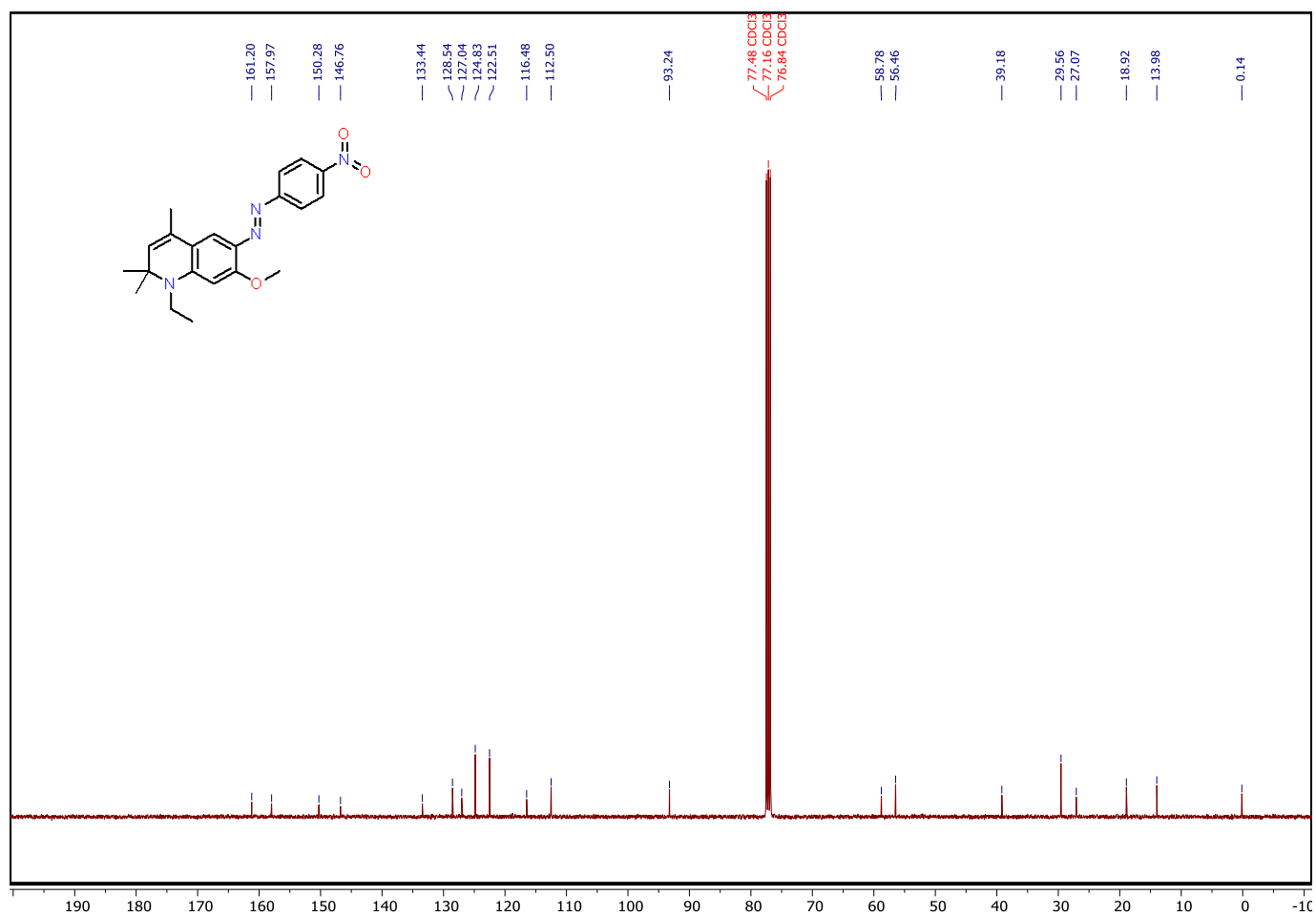


Fig. S44. ^{13}C spectrum of **13**.

^{13}C NMR (101 MHz, CDCl_3) δ 161.20, 157.97, 150.28, 146.76, 133.44, 128.54, 127.04, 124.83, 122.51, 116.48, 112.50, 93.24, 77.48, 77.16, 76.84, 58.78, 56.46, 39.18, 29.56, 27.07, 18.92, 13.98, 0.14.

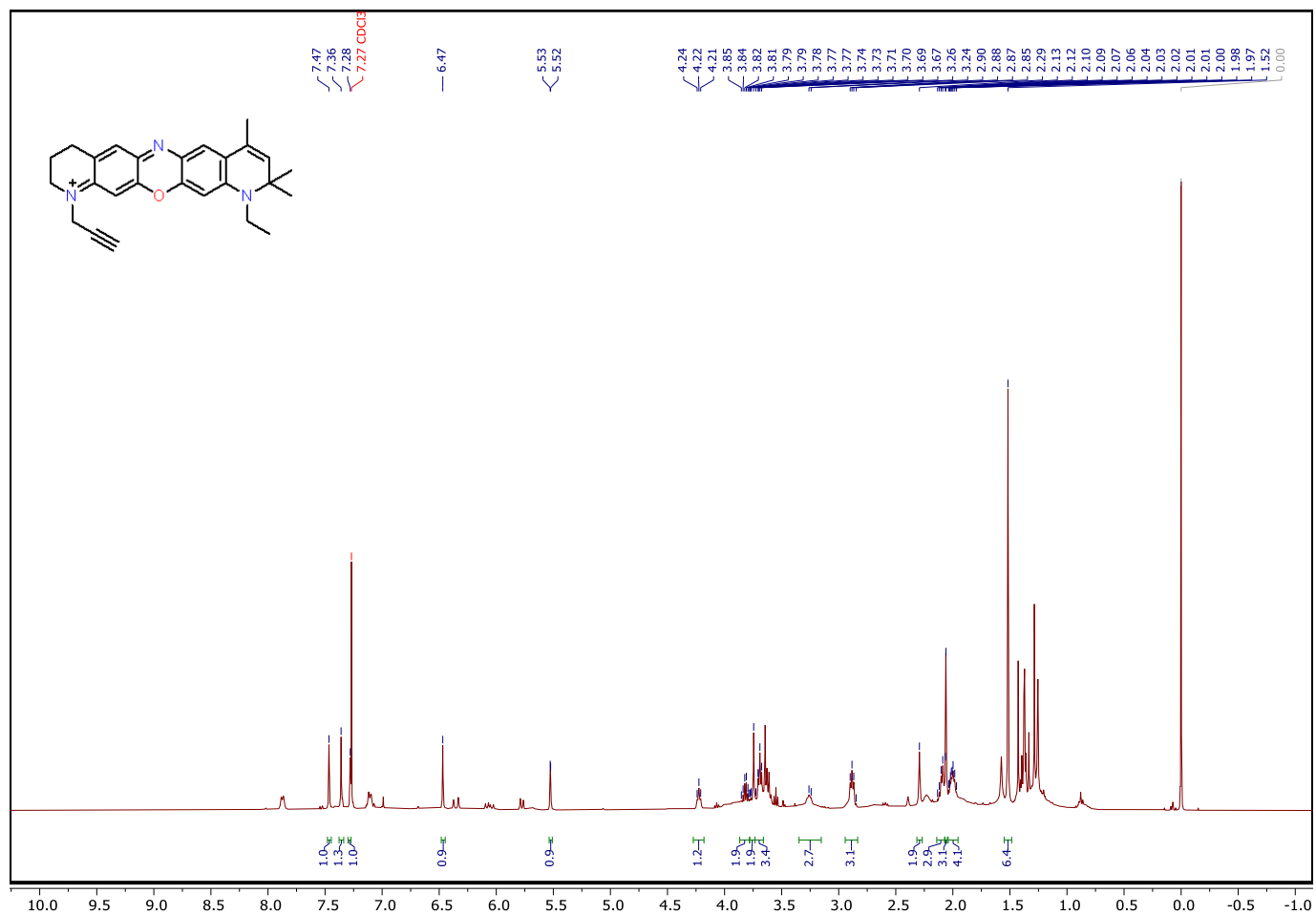


Fig. S45. ¹H spectrum of **14**.

¹H NMR (400 MHz, CDCl₃) δ 7.47 (s, 1H), 7.36 (s, 1H), 7.28 (s, 1H), 6.47 (s, 1H), 5.53 (d, J = 1.5 Hz, 1H), 4.27 – 4.18 (m, 1H), 3.82 (q, J = 5.7 Hz, 2H), 3.74 (s, 2H), 3.73 – 3.66 (m, 3H), 3.25 (d, J = 7.5 Hz, 3H), 2.88 (t, J = 6.3 Hz, 3H), 2.29 (s, 2H), 2.14 – 2.07 (m, 3H), 2.06 (s, 3H), 2.04 – 1.95 (m, 4H), 1.52 (s, 6H).